COMBUSTION CHARACTERIZATION OF BENEFICIATED COAL-BASED FUELS

O. K. Chow, M.J. Hargrove and A.A. Levasseur
ABB POWER PLANT LABORATORIES
Research and Technology
COMBUSTION ENGINEERING, INC.

Contract No. DE-AC 2289 PC 88654

INTRODUCTION

The Pittsburgh Energy Technology Center (PETC) of the U.S. Department of Energy is sponsoring the development of advanced coal-cleaning technologies aimed at expanding the use of the nation's vast coal reserves in an environmentally and economically acceptable manner. Because of the lack of practical experience with deeply beneficiated coal-based fuels, PETC has contracted Combustion Engineering, Inc. to perform a multi-year project on "Combustion Characterization of Beneficiated Coal-Based Fuels."

The objectives of this project include: 1) the development of an engineering data base which will provide detailed information on the properties of Beneficiated Coal-Based Fuels (BCFs) influencing combustion, ash deposition, ash erosion, particulate collection, and emissions; and 2) the application of this technical data base to predict the performance and economic impacts of firing the BCFs in various commercial boiler designs.

The technical approach used to develop the data base includes: bench-scale fuel property, combustion, and ash deposition tests; pilot-scale combustion tests, and full-scale combustion tests. Subcontractors to CE to perform parts of the test work are the Massachusetts Institute of Technology (MIT), Physical Science Inc. Technology Company (PSIT), and the University of North Dakota Energy and Environmental Research Center (UNDEERC).

To date, nine beneficiated coal-based fuels have been acquired through PETC and tested at ABB Power Plant Laboratories Fireside Performance Test Facility (FPTF). These fuels included products from the micro-bubble flotation (Feeley, et al 1987), spherical oil-agglomeration (Schaal, et al 1990) and micro-agglomerate processes.

This paper summarizes the predicted performance and economic impacts of firing the BCFs produced from the micro-bubble flotation and spherical oil-agglomerate processes in coal-fired and oil-fired utility boilers. The combustion test results from firing the beneficiated micro-agglomerate products produced from Illinois No. 5, Pittsburgh No. 8 and Upper Freeport coals in the FPTF are also discussed in this paper.

BOILER PERFORMANCE ANALYSIS AND ECONOMIC IMPACTS

Two utility steam generators designed for either coal- or oil- firing were selected for performance evaluation. The study units were selected to be representative of a large portion of the current boiler population: a 560 MW coal-designed boiler purchased in 1973; and a 600 MW oil-designed boiler purchased in 1970. The schematics of these units are shown in Figure 1. Both of these units were built by ABB/CE, but the fuel related design parameters are similar to those used by other manufacturers.

ABB/CE's Boiler Performance Program (BBP) was used to model the two study boilers. The BPP is a computational tool developed to select various boiler components for new boiler designs and predict

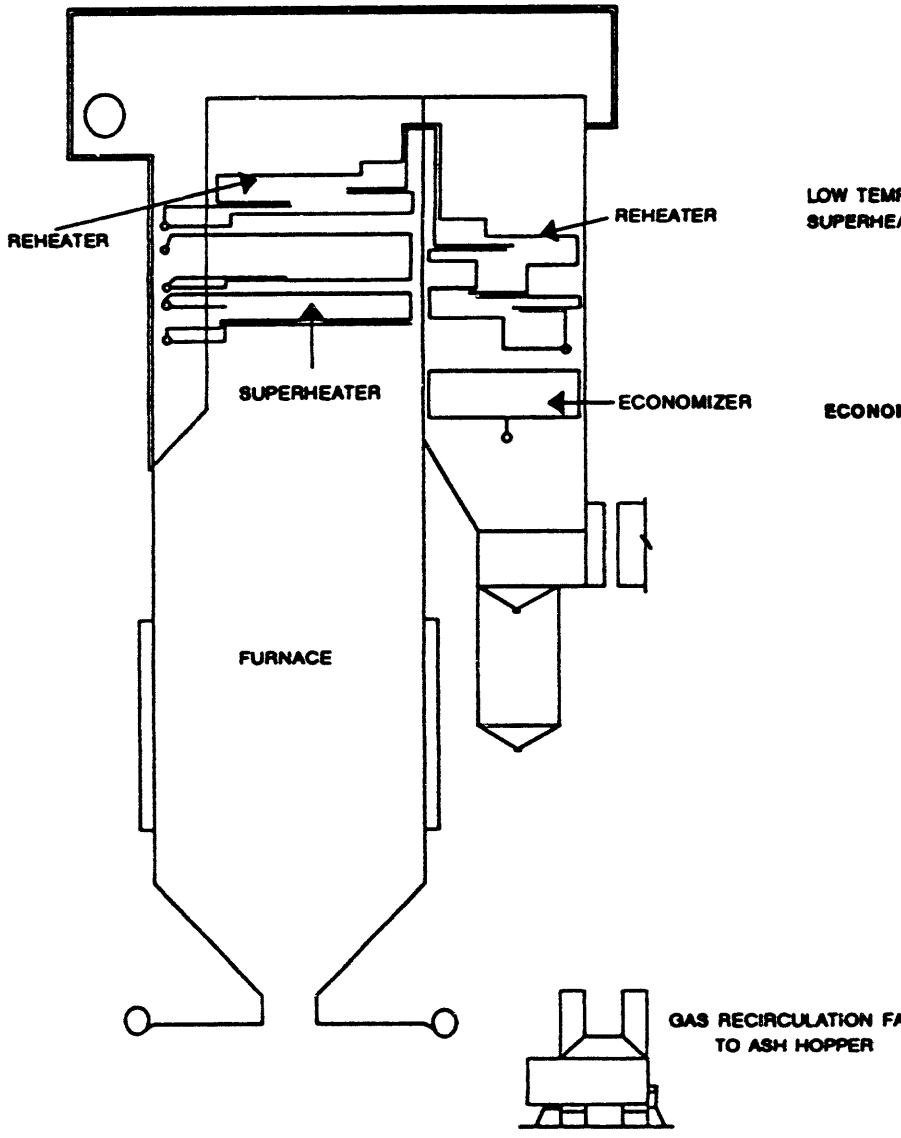

CLOSED-COUPLED SCREEN DESIGN OIL-FIRED
UTILITY STEAM GENERATOR

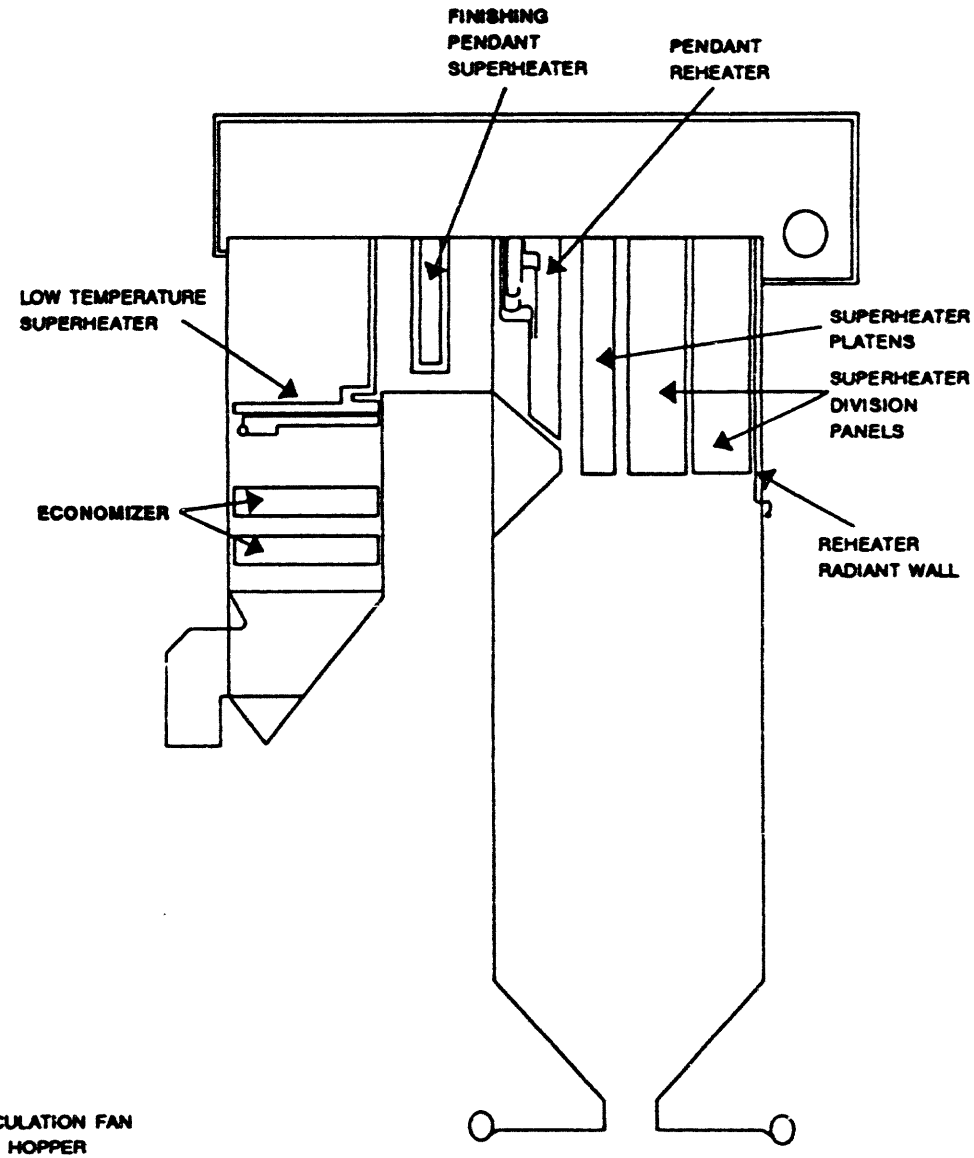

CONVENTIONAL PANEL DESIGN COAL-FIRED
UTILITY STEAM GENERATOR

Figure 1 Schematic of Selected Study Units

the performance of the system. Calculations are performed for the steam generator envelope and related auxiliary equipment which provide information required for detailed component design. The BPP was calibrated with field data which included all known temperatures, pressures and flow rates from the steam and gas sides of the study boiler. The BPP was then used to calculate several parameters that affect boiler heat transfer, including convection pass surface effectiveness and degree of furnace slagging. Once these values were determined, the calculated parameters are used as input along with experimental data to predict boiler performance for the new fuels. The BPP runs in an iterative mode until the fireside and steamside performances balanced.

The fuels evaluated in this study included an Upper Freeport medium volatile bituminous (mvb) parent coal and its Spherical Oil Agglomeration Product (SOAP) at 6% and 25% moisture contents. These fuels were tested in the FPTF to establish slagging, fouling and erosion characteristics (Chow, et. al., 1992). The results provided information required on boiler operating limits. Boiler operating guidelines were established using data from previous studies (Gralton, et. al., 1986, Hargrove, et. al., 1994 and Miemiec, et. al., 1987) and standard engineering boiler design practices. The predicted boiler performance firing the Upper Freeport fuels in the two study units are shown in Table 1.

Overall, the performance analysis indicates the parent coal was the more restrictive fuel, requiring derating in both units. The coal-fired unit showed a 16 percent derating with the parent coal while with the SOAP, the unit capacity could be increased 10 percent over MCR. However, firing the SOAP could not achieve the design superheater and reheater outlet steam temperatures due to the higher thermal conductance in the lower furnace, resulting in greater heat absorption in the furnace and less heat available for absorption in the convection pass.

The oil-designed unit showed significant derating with the Upper Freeport fuels. The derating were a result of convection pass clear spacing. Load was limited by both gas velocity at the Low Temperature Reheat Bank and/or gas temperature at the Lower Superheat Bank.

Firing the BCF in the coal-designed boiler would require little or no modifications. However, firing the BCF in oil-designed boiler would require plant additions and boiler modifications. The retrofit requirements are grouped into the following categories:

- addition of coal receiving and handling systems
- new fuel preparation, feeding and firing system
- boiler modifications
- addition of flue gas desulfurization system
- new particulate removal system
- ash removal and disposal system

The approach for developing capital costs and operating and maintenance (O&M) cost estimates for this coal-fired retrofit were taken from Hargrove, et. al., 1985 with minor modifications where appropriate. This procedure defines the incremental costs and savings as a result of the use of coal as a substitute fuel for oil. The first year incremental operation and maintenance cost savings and the total capital requirement are used to determine a simplified payback period. Also calculated are the total levelized annual revenue savings, specific levelized revenue savings, and the incremental levelized cost of electricity savings. The retrofitted plant is assumed to burn coal, but switches completely to fuel oil at peak demand. This operating mode assumes that the plant is derated on coal or BCF but can regain its maximum capacity when switched to fuel oil.

Plant operating data are used to estimate the cost and savings associated with the retrofit project. In order to compare the fuel oil firing with coal (or BCF) firing on an equal basis, the annual replacement power cost is added to the O&M cost of coal firing. In this way the total yearly kilowatt hours generated are the same for the fuel oil firing and the coal options.

Table 1
Boiler Performance Analyses

PARAMETERS	COAL-FIRED BOILER			OIL-FIRED BOILER		
	PARENT COAL	SOAP25% MOIST.	SOAP 6% MOIST.	PARENT COAL	SOAP25% MOIST.	SOAP 6% MOIST.
Maximum Load, %MCR	84	110	110	43	70	70
Load Limited By	Gas Vel	None	None	Gas Vel	Gas Vel & Clear Space	
Heat Duty, 10^6BTU/h	4171	5119	5090	2276	3554	3553
NHI/PA, 10^6BTU/h/ft^2	1.53	1.92	1.89	1.07	1.66	1.66
Boiler Efficiency, %	89.88	88.04	89.83	89.59	87.08	89.47
Coal Fired, lb/h	367,952	549,828	427,479	201,251	385,228	299,604
Excess Air, %	20	20	20	20	20	20
Gas Recirculation, %	na	na	na	26	6	11.5
Burner Tilt, deg.	-10	+30	+30	+30	-25	-25
Main Steam Flow, lb/h	3,470,000	4,565,000	4,565,000	1,800,000	2,940,000	2,940,000
Reheat Steam Flow, lb/h	3,101,260	4,079,900	4,079,900	1,663,000	2,717,000	2,717,000
Superheater Outlet Temp., °F	1005.0	957.9	959.9	1005.0	1005.0	1005.0
Reheater Outlet Temp., °F	1004.4	960.5	949.5	956.0	957.0	956.0
Lower Furnace Temp., °F	2966	2796	2924	2450	2688	2682
Deposit Conductance, 10^6BTU/h/ft^2/in	20	45	45	41	65	65
Max. Gas Temp. Entering Close Spaced Section, °F	2017	2049	2076	2247	2342	2344
Max. Convection Pass Gas Velocity, ft/s	53	69	66	53	75	76
SH Spray, %	4.6	0.0	0.0	17.4	5.4	4.4
RH Spray, %	0.0	0.0	0.0	0.0	0.0	0.0
Air Heater Inlet Gas Temp. °F	645	696	687	587	643	640
Air Heater Outlet Gas Temp.°F	306	299	316	327	357	351
Air Heater Inlet Air Temp. °F	561	561	579	452	455	454

The costs for producing BCFs fuels in the quantities required for large scale commercial usage are not well established. Also, the fluctuations in oil prices make it difficult to set fuel prices which would be appropriate for this evaluation. For this study differential fuel costs of $1.00, $1.50 and $3.00 have been assumed. These three differential fuel costs have sufficient range so that economic trends can be identified.

Because of the lower capacity factor generally expected when utility units are switched from firing fuel oil 100 percent of the time to firing coal at derated capacity, replacement power will be needed to meet

the plant yearly load demand. The replacement power is assumed to be generated by dispatching other oil-fired units. The cost of replacement power is calculated by assuming the same oil fired net plant heat rate as the study unit and the same variable O&M cost.

The above discussion forms the basis of the annual operating and maintenance cost and savings estimate. The results are the incremental annual O&M costs of coal or BCF firing compared to fuel oil firing. The incremental annual O&M savings thus calculated are used to calculate the total economic impact of a coal conversion over the life of the boiler plant (Figures 2 and 3). The costs associated with capital investment for parent coal or BCF firing would have to be paid back by fuel cost savings. The payback period for both fuels is approximately ten years, based on cost savings of $\$2.0/10^6$-Btu for the parent coal and $\$1.0/10^6$-Btu for BCF, compared to oil.

For the coal-designed unit there are no unit modifications or capital costs required for firing the beneficiated fuels. The basic comparison is therefore a comparison of operating and maintenance costs between firing the parent coal and firing the beneficiated coals. Based on the predicted performance for the unit firing these fuels annual costs were determined and are shown in Table 2.

In developing this table it was assumed the unit would operate for 5000 hours per year. Fuel costs for the beneficiated fuel cases were determined by assuming an equivalent total annual cost for all cases. In this manner the breakeven fuel cost is determined for the beneficiated fuel relative to the parent coal. For this comparison the breakeven fuel cost for the beneficiated fuels is about \$0.07 to $\$0.10/10^6$-Btu greater than for the parent coal.

Table 2
Coal-Designed Unit Economic Evaluation

Operating Parameters	Parent Coal	SOAP 25% Moist	SOAP 6% Moist.
Operating Time, h/year	5,000	5,000	5,000
Net Plant Output, kw	482,018	585,299	588,189
Net Plant Heat Rate, BTU/kwh	9,628	9,681	9,885
Fuel Heat Input, 10^6BTU/yr	23,204,365	28,331,398	29,071,241
Electric Output, 10^6kwh/yr	2,410	2,926	2,941
Replacement Power10^6kwh/yr	516	15	0
Ash Disposal Rate, tons/yr	93,093	52,260	53,608
FGD Disposal Rate, tons/yr	66,228	64,194	66,175
Costs			
Maintenance, $/yr	4,925,000	3,744,000	3,744,000
Ash Disposal, $/yr	930,930	522,600	536,080
Fuel, $/yr	34,806,547	45,458,986	45,638,698
Lime,$/yr	1,865,400	1,808,100	1,863,897
FGD Disposal, $/yr	662,281	641,938	661,749
Replacement Power, $/yr	9,254,266	268,800	0
Total Annual Cost, $/yr	52,444,424	52,444,424	52,444,424
Specific Fuel Cost, $/$10^6$BTU	1.50	1.60	1.57

Figure 2

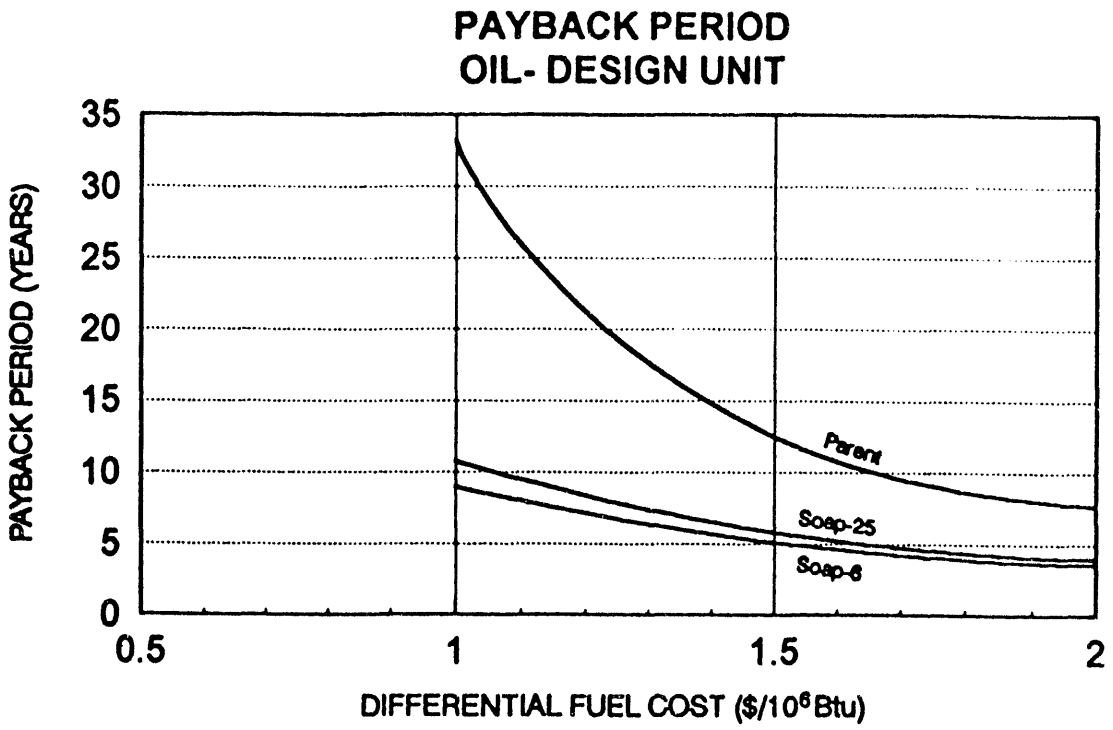

Figure 3

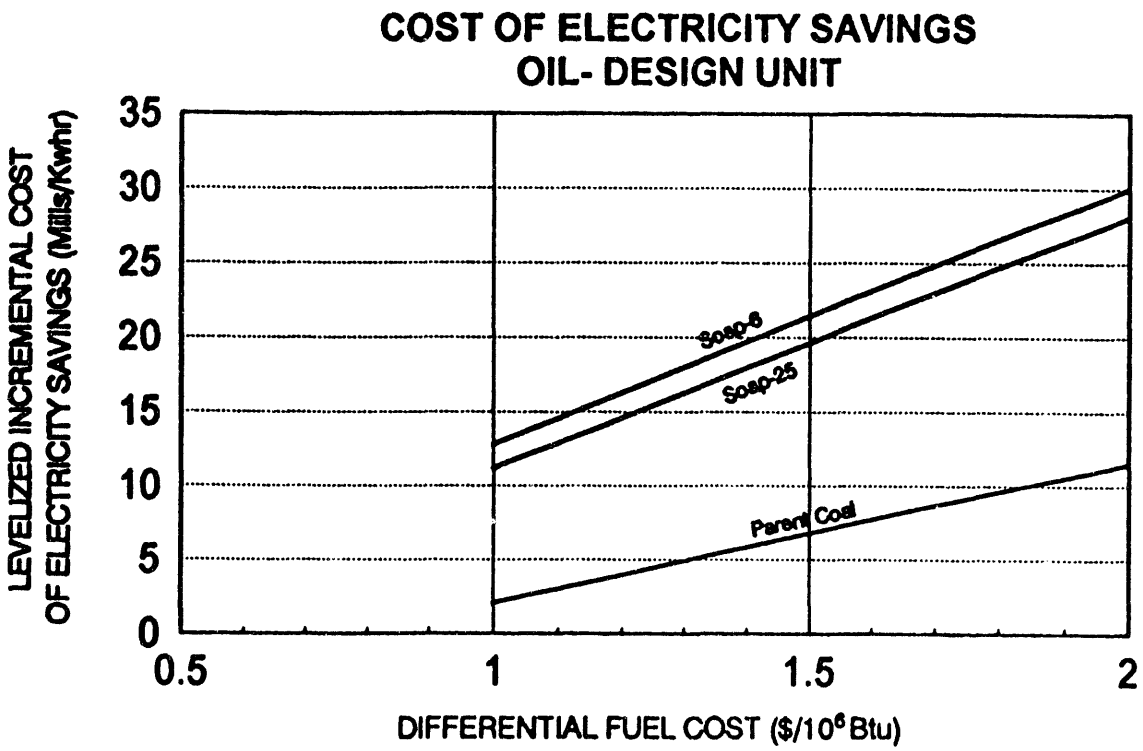

COMBUSTION PERFORMANCE CHARACTERISTICS OF MICRO-AGGLOMERATES

The ASTM analyses of the micro-agglomerates and their respective feed coals are shown in Table 3. The results indicate that the total and pyritic sulfur contents were reduced by 30% to 40% for the Illinois No. 5 and Pittsburgh No. 8, while the Upper Freeport shows no reduction. The ash loadings on a calorific value basis were reduced by 80%, 15% and 29% for the Illinois No. 5, Pittsburgh No. 8 and Upper Freeport products, respectively. The beneficiated products have slightly higher volatile matter contents, perhaps due to the residual diesel oil from the agglomeration process.

Table 3
ASTM ANALYSES OF MICRO- AGGLOMERATE PRODUCTS

Quantity	Illinois No.5		Pittsburgh No.8		UPPER FREEPORT	
	Feed[a]	Product	Feed[b]	Product	Feed[c]	Product
Moisture, wt %	13.2	35.6	4.9	32.5	9.2	27.4
Proximate, wt %						
Volatile Matter	28.7	34.2	34.8	34.7	29.3	30.1
Fixed Carbon	48.4	60.4	58.7	59.9	61.9	63.5
Ash	22.9	5.4	6.5	5.4	8.8	6.4
HHV, Btu/lb	11267	13344	14121	14070	14077	14314
Ultimate, wt %						
Hydrogen	4.5	4.8	5.3	5.2	5.0	5.2
Carbon	63.6	77.1	76.4	79.5	78.7	79.6
Sulfur	2.2	1.4	2.1	1.6	1.2	1.2
Nitrogen	1.0	1.6	1.3	1.4	1.2	1.3
Oxygen	5.7	9.7	8.4	6.9	5.1	6.3
Carbon/Ash	2.8	14.3	11.8	14.7	8.9	12.4
Ash Loading, lb/10^{6}Btu	20.3	4.0	4.6	3.9	6.3	4.5
Sulfur Forms, wt %						
Pyritic	0.91	0.51	0.93	0.59	0.39	0.42
Sulfatic	0.38	0.11	0.08	0.04	0.12	0.12
Organic	0.91	0.78	1.09	0.97	0.69	0.56
Ash Fus. (Red.), °F						
IDT	2080	2010	2090	2010	2080	1930
ST	2120	2040	2120	2100	2250	2030
HT	2270	2100	2230	2150	2300	2130
FT	2380	2200	2400	2250	2540	2310
Ash Comp., wt%						
SiO_2	52.9	42.5	44.3	41.8	46.5	44.5
Al_2O_3	21.2	21.2	24.6	24.5	24.0	24.0
Fe_2O_3	11.8	21.5	19.2	23.5	21.4	20.9
CaO	3.1	3.2	3.5	2.7	1.4	1.7
MgO	1.7	1.4	1.0	1.0	1.0	1.0
Na_2O	0.8	1.2	0.5	0.9	0.4	1.4
K_2O	3.2	2.5	1.3	1.3	2.3	2.4
TiO_2	1.1	1.8	1.2	1.3	1.2	1.4
P_2O_5	0.5	1.0	0.5	0.4	0.3	0.5
SO_3	3.4	3.1	3.7	2.3	1.2	1.3

[a] The Illinois No. 5 coal was from the Wabash Mine, Wabash County, Illinois, AMAX Coal Company. The coal was not cleaned.
[b] The Pittsburgh No. 8 coal was from the Emerald Mine, Greene County, Pennsylvania, Cyprus Coal Company. The coal was pre-cleaned at the mine.
[c] The Upper Freeport coal was from the Sheesley Pit Mine, Jefferson County, Pennsylvania, P&N Coal Company. The coal was pre-cleaned at CQ Inc.

The ash fusion temperatures of the products are generally lower than those of their respective feed coals. The changes for the Illinois No. 5 and Pittsburgh No. 8 are primarily due to changes in base-to-acid constituents of the ash caused by preferential removal of silicate minerals. In the Upper Freeport case, the changes are primarily due to increases in sodium contents, while other ash constituents remained relatively similar. The cause of the sodium increase in the product is not as clear as it is higher than expected from enrichment due to cleaning alone. However, the results from the combustion tests showed there was no discernible difference in ash fouling characteristics between the Upper Freeport product and feed coal.

The as-received beneficiated products have very high moisture (27% to 36% by weight). Initial air-drying was required to facilitate handling. They were then further dried and dispersed into a dry pulverized fuel form using a CE size RP-271 bowl mill. In addition, small batches of Pittsburgh No. 8 and Upper Freeport products at as received moisture were prepared into mulled form by another DOE contractor for testing. The mulling process uses a petroleum-based additive and is supposed to improve the handling characteristics of the products without any drying (Penland, et. al., 1992).

The combination of fines, diesel oil, and in particular, high moisture contents in the micro-agglomerate products had a negative impact on handling. Problems were encountered with the raw coal screw feeder caused by excessive buildup on walls, difficult flow from raw fuel and pulverized fuel storage silos, and minor compaction/pasting inside the bowl mill pulverizer. For a given product, further air-drying (below 16% moisture) alleviated most of these problems.

Processing the Pittsburgh No. 8 and Upper Freeport products into mulled form showed improvements in fuel flow characteristics. Although occasional arching and rat-holing were observed, the products fed through the FPTF fuel handling system with relatively few problems. However, the mulled process did not improve pulverization. The mulled products were still prone to high mill rejection rate and compaction/pasting. Air-drying of the mulled products was required to improve pulverization.

The combustion characteristics of the Illinois No. 5, Pittsburgh No. 8 and Upper Freeport air-dried products at 3.0×10^6 to 4.0×10^6 BTU/h firing rates were good, while the Pittsburgh No. 8 and Upper Freeport mulled products showed occasionally unstable flame at the same firing rates and burner settings. The reason for the unstable flame observed with the Pittsburgh No. 8 and Upper Freeport mulled products is unclear. Analysis of the fly ash samples collected from selected test runs shows the carbon conversions for the mulled products were lower than the air-dried products at either staged and standard firing conditions (Table 4). The results from Thermo-gravimetric analyses indicate similar burn-off rates between the char samples generated from the two mulled fuels and their air-dried product counterparts. The poorer combustion of the mulled products could be caused by poorer fuel dispersions compared to the air-dried products.

Table 4
Combustion Characteristics of Beneficiated Micro-Agglomerate Fuels

Fuel	Form	Firing Rate, 10^6 BTU/h	Firing Mode	Carbon Conversions, %
Illinois No. 5	air-dried	3.0	standard	99.5
		3.0	stage	99.1
Pittsburgh No. 8	air-dried	4.0	standard	99.7
		4.0	staged	99.6
	mulled	4.0	standard	96.8
Upper Freeport	air-dried	3.6	standard	99.6
		3.6	staged	99.3
	mulled	3.6	standard	98.9
		3.6	staged	98.4

The furnace slagging characteristics of the micro-agglomerates are expected to be consistent with those of their respective feed coals. There was little difference in waterwall deposit cleanability between firing the Upper Freeport micro-agglomerate product and its feed coal. Fuel form appeared to have little effect on furnace slagging performance. The results were similar between firing the Pittsburgh No. 8 and Upper Freeport micro-agglomerate air-dried and mulled products. Firing at staged low NOx conditions worsened furnace slagging performance. Furnace deposits developed under these conditions were more tenaciously bonded to the waterwall panels.

The effects of ash deposits on waterwall heat transfer are summarized in Table 3. In all cases, waterwall heat flux recovery was lower at staged than at standard firing under identical firing rate and flame temperature conditions. The more reducing conditions under staged firing affected the transformation of mineral particles in coal by reducing the ash particle viscosity, rendering more tenaciously bonded deposits that are less responsive to soot blowing.

The degradation in furnace performance due to staged firing was fuel dependent. The Upper Freeport fuels were affected the most, followed by Pittsburgh No. 8 fuels, and Illinois No. 5 was the least affected by reduced firing conditions. The critical temperature for removable deposits firing either the Upper Freeport air-dried, mulled products or feed coal was reduced from 2920°F at standard firing to below 2770°F at staged firing conditions. The corresponding temperatures for the Pittsburgh No. 8 micro-agglomerates were 2980°F and 2950°F, respectively. For the Illinois No. 5 micro-agglomerates, these temperatures were approximately 2750°F at standard firing, and below 2750°F at staged firing conditions.

Table 5
Heat Flux Summary of Beneficiated Micro-Agglomerate Fuels

Fuel	Fuel Type	Fuel Form	Firing Rate 10^6 BTU/h	Firing Mode	Furnace Temp., °F	Heat Flux Recovery, %
Illinois No.5	Product	Air-dried	3.0	Standard	2750	67
			3.2		2850	14
			3.6		2920	0
			3.0	Staged	2740	55
Pittsburgh No. 8	Product	Air-dried	3.6	Standard	2910	80
			4.0		2980	66
			4.0	Staged	2950	41
		Mulled	4.0	Standard	2950	70
Upper Freeport	Feed	Dried	3.4	Standard	2840	56
			3.6		2900	50
			3.1	Staged	2760	63
			3.2		2840	44
			3.6		2900	34
	Product	Air-dried	3.4	Standard	2820	66
			3.6		2920	54
			3.1	Staged	2770	53
			3.2		2850	28
			3.6		2920	0
	Product	Mulled	3.4	Standard	2860	70
			3.6		2910	61
			3.1	Staged	2780	53

The FPTF results showed all test fuels had low fouling potentials at the gas temperature range tested (2200°F to 2450°F). The deposit buildup rates in the convective pass were low. Soot blowing was not required over a 12-hour period. Deposits developed were sintered, and could be easily removed from the tube surfaces. There was minimal difference in fouling characteristics between firing the air-dried or mulled products under standard or staged low NOx firing conditions.

The relative deposit removability is measured on-line in the FPTF with a penetrometer. Typically, based on the correlations established between the FPTF and field, deposit bonding strengths up to 15 are considered controllable by conventional soot blowing. The results from the FPTF test runs indicate that, at 2200°F to 2450°F gas temperatures, all three micro-agglomerate products had deposit bonding strengths below 10.

CONCLUSIONS

Based on the bench-scale and pilot-scale test results and the analysis approach, the selected BCF's can be fired in the two study units with good results. The BCF's perform significantly better than their Upper Freeport parent coal. The oil-designed unit would require substantial capital investment for parent coal or BCF firing, which would have to be paid back by fuel cost savings. The payback period for both fuels is approximately ten years, based on cost savings of $\$2.0/10^6$-BTU for the parent coal and $\$1.0/10^6$-BTU for BCF, compared to oil. The coal-designed unit would not require significant investment, and load capability would increase. However, the breakeven beneficiation cost would be only $\$0.1/10^6$-Btu.

The combustion test results indicate that the beneficiated micro-agglomerate fuels produced from Illinois No. 5, Pittsburgh No. 8 and Upper Freeport can effectively be burned under conditions representative of commercial furnaces. However, the high moisture contents in these fuels can present handling problems. Processing the products into mulled form improved storage and flowing characteristics, but the high moisture still caused problems during pulverization.

Furnace slagging characteristics of the micro-agglomerates are expected to be consistent with those of their respective feed coals. Firing under staged low NOx conditions worsened furnace slagging. The degradation in performance was fuel dependent. All test fuels exhibited low fouling propensity at the gas temperature range tested. The mulling process appeared to have little impact on the combustion performance of these fuels.

REFERENCES

Chow, O.K., Nsakala, N, Levasseur, A. A., Hargrove, M. J. "Fireside Combustion Performance Evaluation of Beneficiated Coal-Based Fuels", 92-JPGC-FACT-1, October, 1992.

Gralton, G. W., Beal, H. R., Hargrove, M. J., and Levasseur, A. A., "Retrofit Evaluations of Standard Grind and Fine Grind Coal-Water Fuels," Eighth International Symposium on Coal Slurry Fuels Preparation and Utilization, May 27-30, 1986, Orlando, Florida.

Hargrove, M. J., Liljedahl, G. N., "Coal-Water-Slurry Technology Development, Volume 2: Conversion Guidelines", EPRI Report CS-3374, March 1985.

Hargrove, M., Gurvich, B., Kwasnik, A., Liljedahl, G., Miemiec, L. "Predictions of Boiler Performance When Firing Beneficiated Coal-Based Fuels", Proceedings of the 19th International Technical Conference on Coal Utilization and Fuel Systems, March, 1994

Miemiec, L. S., Lexa, G. F., Levasseur, A. A., Mehta, A. K., "Effects of Coal Cleaning on Boiler Performance", ASME Paper 87-JPGC-FACT-7, October 1987.

Penland, R.K., Davis, B.E., and Singleton, A.H. "Commercial Applications for Mulled Coal Technology", Proceedings of the 17th International Conference on Coal Utilization & Slurry Technology, April, 1992.

UTILIZATION OF COAL-WATER FUELS IN FIRE-TUBE BOILERS

D. K. MORRISON, DESIGN ENGINEER
T. A. MELICK, PROJECT ENGINEER
T. M. SOMMER, VICE PRESIDENT
Energy and Environmental Research Corporation
1345 N. Main Street
Orrville, Ohio 44667
(216) 682-4007

ABSTRACT

The Energy and Environmental Research Corporation (EER), in cooperation with the University of Alabama and Jim Walter Resources, was awarded a DOE contract to retrofit an existing fire-tube boiler with a coal-water slurry (CWS) firing system. Recognizing that combustion efficiency was the principle concern when firing slurry in fire-tube boilers, EER focused the program on innovative approaches for improving carbon burnout without major modifications to the boiler. The project was completed in April 1994.

The boiler was successfully operated on coal-water slurry for 800 hours. A boiler derate of 20 percent was necessary for successful operation with slurry accounting for 62 percent of the total heat input with the balance provided by natural gas. Under these boiler conditions, the carbon conversion was 90 percent. The economics of slurry firing in fire-tube boilers is also presented in this paper.

INTRODUCTION

In the industrial and commercial markets, fire-tube boilers represent the major portion, about 70 percent, of small oil- and gas-fired boilers. Annually, these boilers consume approximately ten percent of the total energy used in the combined industrial and commercial market sectors. Thus, replacing the premium fuels now used in these markets with coal-based fuels would accomplish a significant reduction in oil and gas consumption.

Water-tube boilers predominate in large industrial and utility applications and, as the name implies, are designed differently than fire-tube boilers. In water-tube units, the combustion gases flow outside and around tubes filled with water that is heated to produce steam. In fire-tubes, however, heat is transferred from hot combustion gases flowing inside tubes to water contained in a shell that surrounds the tubes.

Because the shell of a fire-tube boiler must withstand the pressure of the steam produced, high pressures and large boiler sizes (i.e., large shell diameters) would require extremely thick shell walls. Thus, fire-tube boilers usually have smaller capacities than water-tube units.

These two types of designs result in different gas flow patterns, velocities, and temperature profiles, which lead to differences in heat transfer characteristics and other performance factors

that affect system efficiency and durability. Over the last 15 years, a substantial amount of work has been conducted on slurry fuels that were predominately fired in water-tube boilers. A range of slurries has been developed and field evaluations have been conducted on several boilers, and industrial equipment world wide. Much of the technology required to fire slurries in fire-tube boilers already exists including slurry preparation, slurry storage and handling, burners and approaches to handling the coal ash.

The key problem in firing slurries in fire-tube boilers designed for gas or oil firing is the extremely short combustion zone residence time available. In addition, fire-tube designs incorporate a long, narrow combustion chamber with no refractory lining which promote rapid cooling of the combustion products. Conventional slurry firing experience, used for larger systems designed to accommodate lower combustion intensities, is not directly applicable to fire-tubes. There is simply not enough volume in the fire-tube to complete combustion of the coal without utilizing additional combustion enhancements or, consequently, derating the boiler.

To determine the feasibility of converting such a boiler, the Energy Department's Pittsburgh Energy Technology Center funded this project with EER to retrofit a 3.8 million Btu/hr Cleaver-Brooks fire-tube boiler at the University of Alabama. The Mining Division at Jim Walter Resources, Inc. prepared and delivered slurry to the University. The results of this program combined with results from on going water-tube boiler tests, provide a broad data base that can be applied to virtually all commercial and industrial boilers.

PROGRAM

The program consisted of five tasks. Task 1 provided for the design and retrofit of the host boiler to fire coal-water slurry. Task 2 was a series of optimization tests that determined the effects of adjustable parameters on boiler performance. Task 3 provided about 1000 hours of proof-of-concept system tests. Task 4 was a comprehensive review of the test data in order to evaluate the economics of slurry conversions. Task 5 could have provided for the decommissioning of the test facility if required.

BOILER CHARACTERISTICS

The host boiler is located on the University of Alabama Campus in Tuscaloosa, Alabama. It is a Cleaver-Brooks Model LF-211X-8, 4 pass, 80 hp fire-tube boiler rated at 2,816 lbs/hr of steam at 150 psig. At it's rated capacity, the gas firing rate is approximately 3.8 million Btu/hr. It was installed in 1950, and has 352 square feet of heating surface. The boiler was designed to be fired with either fuel oil or natural gas but has fired only natural gas. Since the boiler is designed to fire only gas or oil, it was not equipped with particulate removal equipment, sootblowers, compressed air, or an air heater. The boiler is connected to the University's main steam supply system. The boiler is of the "dry back" variety, indicating that the rear wall is not water-cooled.

BOILER RETROFIT

The retrofit equipment included a CWS supply system, CWS burner, combustion air and flue gas handling equipment, sootblowers, air compressor, and control system. CWS was delivered to the site by tank truck. Slurry unloading from the truck was accomplished with an air operated diaphragm pump into a 4500 gallon storage tank. The tank is equipped with a mixer and a containment wall. Slurry flows from the tank to the slurry pump which increases the slurry pressure to 150 psig. Following the pump, a basket strainer and mass flow meter were installed. A slurry heater was installed in the system but was by-passed due to problems with viscosity increasing as the slurry was heated. The CWS burner designed by EER utilized a narrow angle refractory quarrel to improve CWS ignition stability. The CWS burner is also capable of firing natural gas at it's rated capacity. The CWS twin fluid atomizer utilizing compressed air operated in the range of .65 to .95 air to fuel ratio. The retrofit also included the installation of new FD and ID fans along with an air heater, particulate collection cyclone, and baghouse. The cyclone was used to capture the larger, carbon containing particles for reinjection into the combustion chamber. The boiler was equipped with air sootblowers to control ash deposition in the tubes. An air compressor was installed to provide air for the sootblowers and slurry atomization. The boiler was equipped with automatic controls for most of the boiler functions. Since the system was operated as a test facility, a boiler operator was required by the University to be on site during boiler operation.

RESULTS

EER's design approach focused on increasing carbon conversion during CWS firing. Air preheating, refractory lining, and natural gas co-firing had a positive effect on carbon conversion. Ash recycle was used to reinject the large carbon containing particles that were captured in the cyclone back into the boiler for additional time at combustion temperature.

Air Preheat

A series of tests were performed to determine the overall increase in boiler efficiency due to the effect of combustion air preheat. The average efficiency increase due to combustion air preheat was 2 percent over the load range of 50-100 percent. Heat transfer surface area increased 250 percent with the addition of the air preheater. This test was preformed using natural gas. Tests varying the air preheat temperatures were also preformed while firing CWS but required natural gas flows were unacceptable.

Refractory Length

Thermal modelling indicated that the fire-tube should be lined with 24 inches of refractory in addition to the 15 inch long refractory throat to maintain a higher combustion zone temperature. By accident the fire-tube was retrofitted with a 3 foot refractory liner. During the initial

operation of the boiler, slag began to form in the throat of the fire-tube. This molten slag began to accumulate at the end of the refractory liner. It was decided to shorten the refractory liner to 1 foot. Due to this change, the carbon conversion dropped from 95 percent to 87 percent and the boiler efficiency dropped from 79 percent to 74 percent. However, by shortening the refractory, the slagging in the fire-tube was eliminated.

Ash Recycle

Flyash recycle was investigated as a means of reducing carbon losses. A baseline test was performed with all of the ash going to the baghouse. The ash that was collected in the cyclone was injected into the baghouse by the venturi eductor. The second test was identical to the first test with the exception that the cyclone ash was recycled into the boiler. The carbon in the ash dropped from 69 percent to 54 percent and the carbon conversion increased from 73 percent to 86 percent. The boiler efficiency increased from 66 percent to 73 percent. The ash was analyzed for carbon content as a function of particle size. For particles larger than 75 microns the carbon content was 80%, for particles between 38 and 75 microns 76%, and for particles smaller than 38 microns the carbon content was 54%. In addi' on to the above test, cyclone and baghouse samples were collected over a wide range of slurry and natural gas flows. The natural gas flow rate varied from 700 scfh to 1250 scfh and the slurry flow rate varied from 100 #/hr to 200 #/hr. The carbon content of the cyclone catch was an average 15 percent higher than the ash in the baghouse.

Natural Gas Support

The boiler was warmed by firing natural gas only. CWS firing was initiated when the air preheat temperature of 400°F was obtained. The natural gas flow rate was reduced as the CWS flow rate was increased to maintain a constant boiler load.

The effect of supplementary firing of natural gas was also evaluated during this test series: samples were taken at the cyclone outlet and at the baghouse and analyzed for carbon content. The highest carbon conversion measured was 92 percent. This was obtained while firing 1100 scfh natural gas and 125 #/hr slurry. These flow rates equate to 60 percent boiler load and 52 percent of the thermal input as slurry.

Maximum boiler load achieved was 80 percent when firing CWS. CWS accounted for 62 percent of the total heat input. Boiler loads did not exceed 80 percent due to a decrease in carbon conversion resulting from reduced residence time and baghouse inlet flue gas temperature restrictions. The highest heat input due to CWS occurred at 200 #/hr slurry and 700 scfh gas flow. The boiler load was 70 percent under these conditions with CWS accounting for 72 percent of the heat input. Carbon conversion decreased to 87 percent.

The boiler was operated at 150 #/hr slurry corresponding to a boiler load of 38 percent with no gas support for a period of 5-10 minutes on two different occasions. The test was terminated due to a loss in air preheat temperature and combustion stability. The test took place with the 3 foot refractory configuration.

ECONOMICS

An advanced coal based system will require a larger initial investment than a comparable gas or oil fired boiler. To be attractive to a potential customer, differential operating and maintenance costs must be sufficiently low, such as to offset the higher initial investment and provide net overall cost savings over a reasonable time. To determine which parameters are necessary to create an attractive payback period, the economics of converting an oil or gas fired boiler to CWS was evaluated.

The operating costs of the existing gas or oil fired boiler were calculated. The new operating costs and the total plant investment to add slurry firing was then calculated and compared. The analysis was performed by varying the fuel costs, capacity factor, and capacity of the boiler. The analysis was based upon the simple payback period method of evaluating investment decisions. Payback period is the length of time required for an investment to pay for itself, payback occurring when cumulative net cash inflows produce savings or gross profit to the owner.

Fuel costs of 4, 5, and $6/MMBtu were used for natural gas and 5, 6, and $7/MMBtu for #2 oil. Boiler capacities utilized were 2,800, 4,000, 10,000, and 28,000 lb/hr steam. Based on the 20% boiler derate, capacity factors of 64, 48, and 32 percent were used. Also considered was whether the slurry system was being retrofitted to an existing boiler, installed on one (1) new boiler, or being installed on a new boiler in large quantities.

The results of the economic analysis are that boilers smaller than 4,000 lb/hr steam are not good candidates for conversion unless they are shop assembled in large quantities (greater than 10). Boilers in the 4,000 to 10,000 lb/hr range become attractive for retrofit if they are subject to high fuel cost differentials and capacity factors. Most boilers larger than 10,000 lb/hr steam have short payback periods and are excellent candidates for conversion to coal water slurry. Tables 1 & 2 illustrate the payback period for retrofitting gas and oil fired boilers. Tables 3 & 4 illustrate the payback period when comparing a boiler retrofit, one new boiler, and high volume production for gas and oil gas fired boilers.

CONCLUSIONS AND RECOMMENDATIONS

The boiler has been successfully operated firing coal-water slurry for extended periods of time with few slurry related operational problems. The following performance goals were met; fully automatic start-up, coal water slurry as the primary fuel, natural gas as the secondary fuel, turndown of 3:1, reliability/safety comparable to oil fired boilers, automatic dust-free ash

removal, scheduled maintenance less than twice a year, service life of the overall system greater than 20 years, and local emissions compliance. The following performance goals were not met. Combustion efficiency was projected to be >99 percent, maximum obtained during testing was 95 percent. Thermal efficiency was projected to >80 percent, maximum obtained during testing was 79 percent. The projected routine operating/maintenance labor requirements were 7 hours a week. We now anticipate this to be 13 hours.

Retrofitting an existing oil or gas fired boiler to slurry becomes economical when the boiler capacity is more than 10,000 lb/hr steam when using 1994 fuel costs. If the fuel cost differential increases in the future the minimum boiler size will decrease. When considering new boiler systems or new boiler systems produced in large quantities, the economics look attractive for boilers in the 4,000-10,000 lb/hr range.

Improving carbon burnout is the most significant area that will make the economics more attractive and convince boiler owners to convert to firing coal water slurry. This program did not allow for any modifications to the furnace volume, however, the heat transfer modelling clearly showed that adequate first pass temperature and residence time are required to achieve high carbon conversion. The population of fire-tube boilers simply cannot provide adequate residence time for coal combustion and achieve 99% carbon conversion. Many units however, could be retrofit with small pre-combustion chambers to achieve this goal.

EER believes that this concept could be demonstrated in a very cost effective manner utilizing the facilities and information resulting from this program. The predicted enhancements of the precombustor are as follows:

- Improve carbon burnout
- Improve combustion efficiency
- Reduce the payback period
- Eliminate 80% of the ash in the boiler
- Reduce the NO_x emissions
- Eliminate support fuel
- Remove ash collecting and recycling equipment

The precombustor will improve the ability to offer a commercial product that will compete with oil and gas fired boilers.

ACKNOWLEDGMENT

This work has been sponsored by the Department of Energy (Pittsburgh Energy Technology Center) under the Contract No. DE-AC22-90PC90165 under the direction of John C. Winslow.

TABLE 1. FIRE-TUBE BOILER ECONOMIC SUMMARY
Natural Gas Fired Boiler

Boiler Rated Capacity	N.G. cost	Slurry cost	Payback period in years		
in #/hr	$/mmbtu	$/mmbtu	32%cf	48%cf	64%cf
4000	4	1.5	-	-	-
4000	5	1.5	-	-	-
4000	6	1.5	-	15.31	9.99
10000	4	1.5	-	14.69	9.64
10000	5	1.5	12.45	7.14	5.01
10000	6	1.5	7.79	4.72	3.38
15000	4	1.5	15.67	8.68	6.00
15000	5	1.5	7.95	4.80	3.44
15000	6	1.5	5.32	3.32	2.41
28000	4	1.5	8.06	4.86	3.48
28000	5	1.5	4.68	2.94	2.14
28000	6	1.5	3.29	2.11	1.55

- means that the payback period exceeds 20 years
cf = capacity factor based on the derated boiler load

TABLE 2. FIRE-TUBE BOILER ECONOMIC SUMMARY
Oil Fired Boiler

Boiler Rated Capacity	OIL cost	Slurry cost	Payback period in years		
in #/hr	$/mmbtu	$/mmbtu	32%cf	48%cf	64%cf
4000	5	1.5	-	-	-
4000	6	1.5	-	15.17	9.91
4000	7	1.5	17.70	9.59	6.58
10000	5	1.5	12.33	7.09	4.97
10000	6	1.5	7.75	4.69	3.39
10000	7	1.5	5.65	3.51	2.54
15000	5	1.5	7.89	4.77	3.42
15000	6	1.5	5.30	3.30	2.40
15000	7	1.5	3.99	2.53	1.85
28000	5	1.5	4.65	2.92	2.13
28000	6	1.5	3.28	2.10	1.54
28000	7	1.5	2.53	1.63	1.21

- means that the payback period exceeds 20 years
cf = capacity factor based on the derated boiler load

TABLE 3. FIRE-TUBE BOILER ECONOMIC SUMMARY
Natural Gas Fired Boiler

Boiler Rated Capacity	N.G. cost	Slurry cost	Payback period in years		
in #/hr	$/mmbtu	$/mmbtu	retrofit	new	high volume
4000	4	1.5	-	-	-
4000	5	1.5	-	-	9.59
4000	6	1.5	15.31	10.86	5.27
10000	4	1.5	14.69	10.32	5.73
10000	5	1.5	7.14	5.28	3.13
10000	6	1.5	4.72	3.55	2.15
15000	4	1.5	8.68	6.32	3.87
15000	5	1.5	4.80	3.60	2.28
15000	6	1.5	3.32	2.51	1.61
28000	4	1.5	4.86	3.62	2.44
28000	5	1.5	2.94	2.22	1.52
28000	6	1.5	2.11	1.60	1.10

- means that the payback period exceeds 20 years
Economic analysis performed at 48% capacity factor

TABLE 4. FIRE-TUBE BOILER ECONOMIC SUMMARY
Oil Fired Boiler

Boiler Rated Capacity	OIL cost	Slurry cost	Payback period in years		
in #/hr	$/mmbtu	$/mmbtu	retrofit	new	high volume
4000	5	1.5	-	-	9.47
4000	6	1.5	15.17	10.78	5.23
4000	7	1.5	9.59	7.05	3.61
10000	5	1.5	7.09	5.24	3.11
10000	6	1.5	4.69	3.53	2.14
10000	7	1.5	3.51	2.66	1.63
15000	5	1.5	4.77	3.57	2.26
15000	6	1.5	3.30	2.50	1.61
15000	7	1.5	2.53	1.92	1.25
28000	5	1.5	2.92	2.21	1.51
28000	6	1.5	2.10	1.60	1.10
28000	7	1.5	1.63	1.25	0.86

- means that the payback period exceeds 20 years
Ecomonic analysis performed at 48% capacity factor

ENVIRONMENTAL CONTROL POSTER SESSION

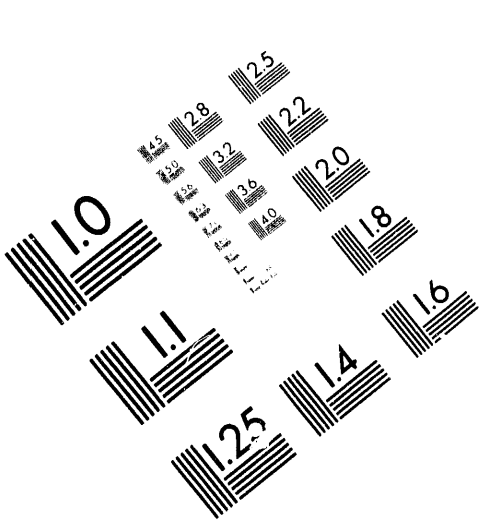

Association for Information and Image Management

1100 Wayne Avenue, Suite 1100
Silver Spring, Maryland 20910

301/587-8202

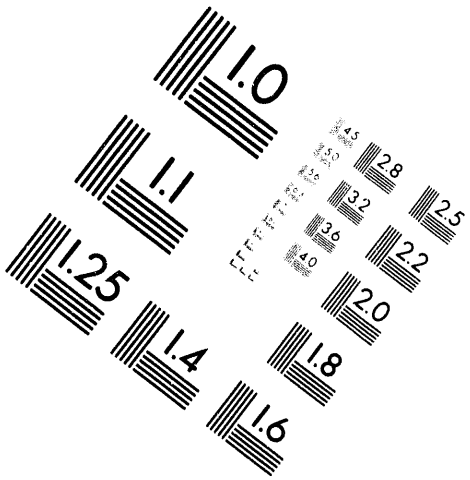

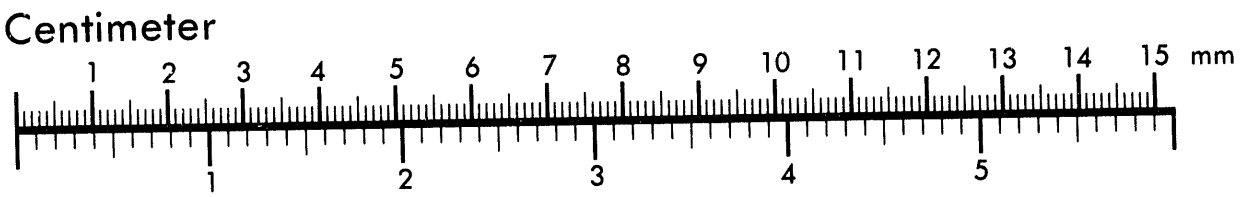

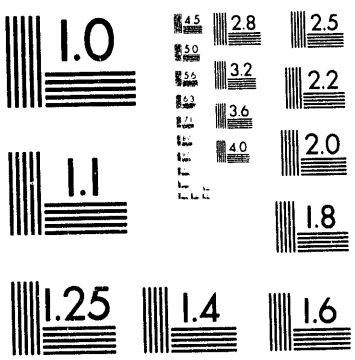

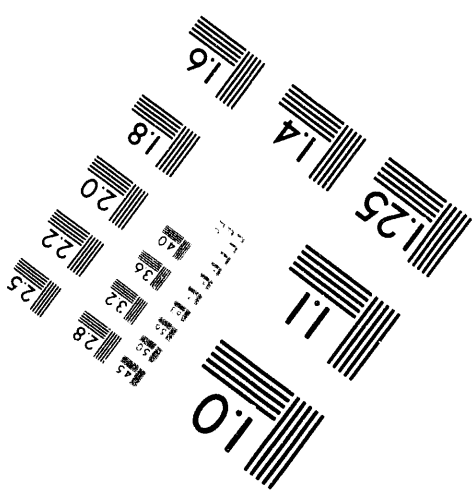

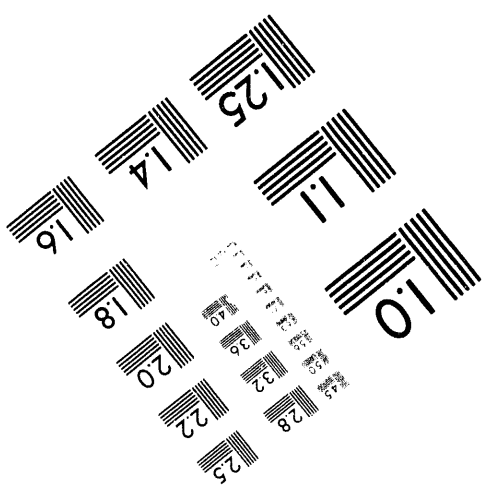

MANUFACTURED TO AIIM STANDARDS
BY APPLIED IMAGE, INC.

3 of 4

DEVELOPMENT OF THE INTEGRATED ENVIRONMENTAL CONTROL MODEL: UPDATE ON PROJECT STATUS

E.S. Rubin, M.B. Berkenpas, J.R. Kalagnanam and H.C. Frey
Carnegie Mellon University
Pittsburgh, PA 15213

INTRODUCTION

This paper describes the Integrated Environmental Control Model (IECM), an analytical model developed for the U.S. Department of Energy's Pittsburgh Energy Technology Center (DOE/PETC) [1,2]. Model development work is continuing under a new contract initiated in October 1992. The model quantifies the performance and cost of power plant designs that involve user-specified combinations of pre-combustion, combustion, and post-combustion methods of environmental control. A unique feature of the IECM is the ability to characterize uncertainty in probabilistic terms, in contrast to conventional deterministic analysis. This capability offers special advantages in analyzing advanced technologies at an early stage of development , and in comparing them with conventional systems where uncertainties typically are smaller. This paper reviews the current status of model development and plans for further refinements, testing and applications.

MODEL OVERVIEW

Figure 1 shows the technologies currently included in the Integrated Environmental Control Model. These include a number of commercially available methods of pollution control, as well as several advanced technologies of interest to DOE/PETC. For each of the technologies listed in Figure 1, a process performance model was developed to account for mass and energy flows associated with that process. Coupled to each performance model, an economic model also was developed to estimate the capital cost, annual operating cost and total levelized cost of each technology. Details of the performance and cost models originally developed for the IECM have been reported elsewhere [1, 2].

Running the IECM involves three principal steps. The first is to configure a power plant for analysis. Here, the user specifies the set of pre-combustion, combustion, and post-combustion technologies of interest, along with associated waste disposal or byproduct recovery methods. Next, the user specifies the values of model parameters related to control technology design, power plant characteristics, fuel specifications, and environmental regulatory constraints. Economic and financial parameters also are specified at this stage. Overall, the IECM contains several hundred input parameters covering all technologies in the model. For a typical analysis, on the order of 50 parameters must be specified. Default values for most parameters are incorporated to assist the

Figure 1. Integrated Environmental Control Model Technologies

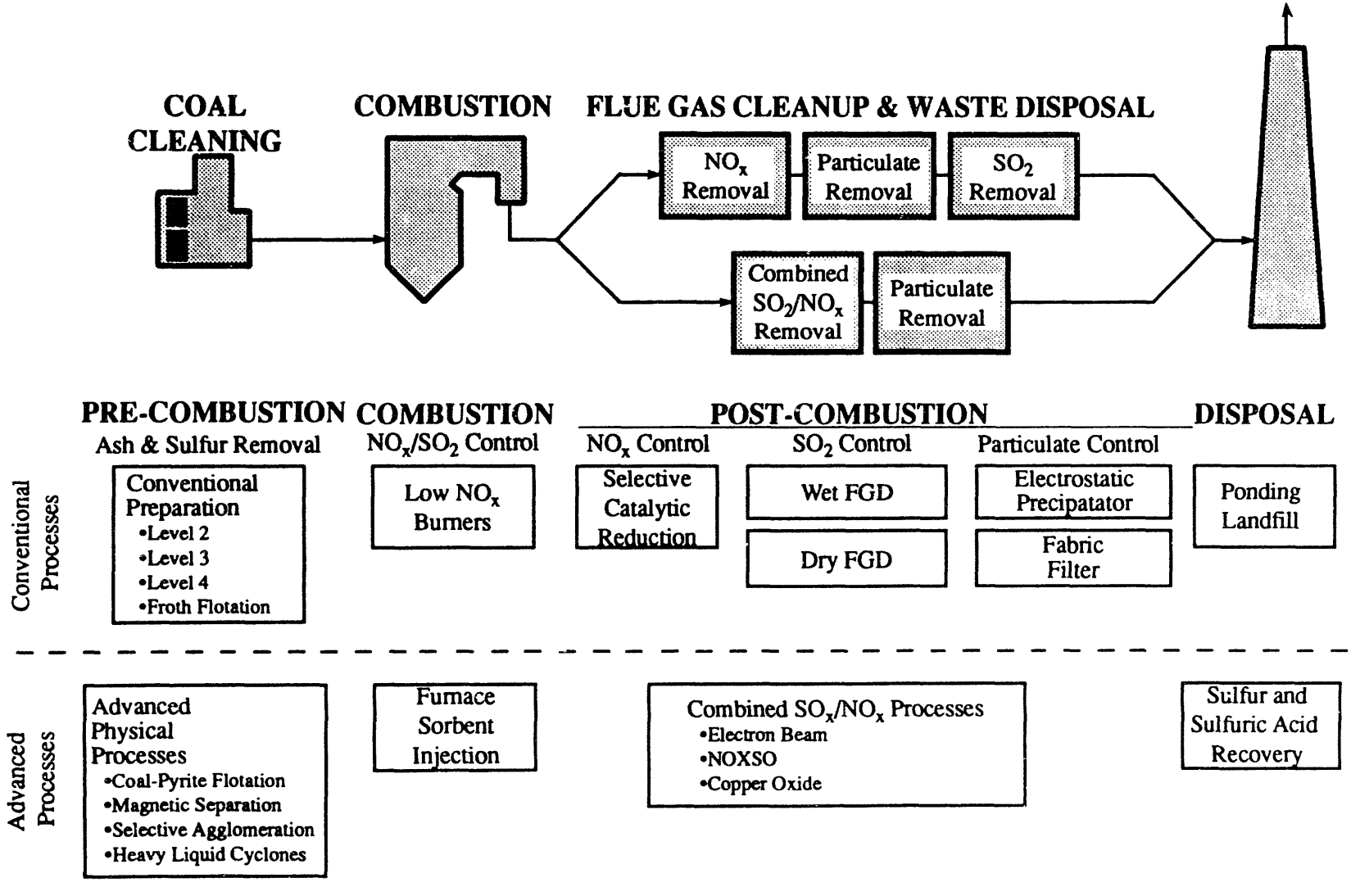

user. Finally, once all input parameters are set, the model is executed and the desired output results are specified. Several standard reports are incorporated for economic analysis, though the user may easily call for any performance or economic output parameter of interest.

The model runs on a Macintosh II computer. As discussed later, a particular advantage of the Macintosh system is its capability to support a user-friendly graphical interface to facilitate model use.

Probabilistic Capability

As noted earlier, a unique feature of the IECM is its ability to characterize input parameters and output results probabilistically, in contrast to conventional deterministic (point estimate) form. This method of analysis offers a number of important advantages over the traditional approach of examining uncertainties via sensitivity analysis. Probabilistic analysis allows the interactive effects of variations in many different parameters to be considered simultaneously, in contrast to sensitivity analysis where only one or two parameters at a time are varied, with all others held constant. In addition, probabilistic analysis provides quantitative insights about the *likelihood* of certain outcomes, and the probability that one result may be more significant than another. This type of information is generally of greater use than simple bounding or "worst case" analyses obtained from sensitivity studies, which contain no information on the likelihood of worst case occurrences.

The ability to perform probabilistic analysis comes from the use of a new software system which uses a non-procedural modeling environment designed to facilitate model building and probabilistic analysis [3]. In addition to a number of standard probability distributions (e.g., normal, lognormal, uniform, chance), the IECM can accommodate any arbitrarily specified distribution for input parameters. Given a specified set of input uncertainties, the resulting uncertainties induced in model outputs are calculated using median Latin Hypercube sampling, an efficient variant of Monte Carlo simulation. Results typically are displayed in the form of a cumulative probability distribution showing the likelihood of reaching or exceeding various levels of a particular parameter of interest (e.g., cost). Examples of model results have been presented previously [1, 4].

Model Applications

The IECM is intended to support a variety of applications related to technology assessment, process design, and research management. Examples of questions that can be addressed with the IECM include the following:

- What uncertainties most affect the overall costs of a particular technology?
- What are the key design trade-offs for a particular process ?

- What are the potential payoffs and risks of advanced processes vis-a-vis conventional technology?
- Which technologies appear most promising for further process development?
- What conditions or markets favor the selection of one system design (or technology) over another?
- How can technical and/or economic uncertainties be reduced most effectively through further research and development?

Various case studies have been undertaken using the IECM to address questions like these [5,6,7]. Additional applications are planned under the current project, as discussed below.

SCOPE OF CURRENT WORK

Version 1.0 of the Integrated Environmental Control Model was transferred to DOE/PETC in 1991 [2,8]. Under the new contract initiated in October 1992, twelve new tasks, organized into two project phases, will be pursued to update and enhance the IECM. Details of these tasks have been elaborated in a project management plan [9].

Initial efforts included an on-site training program for PETC personnel on the use of both the IECM and the Demos programming language. The latter capability is necessary for developing new models, or making significant revisions to existing ones. The training program was initiated in February 1993 and will continue on an intermittent basis throughout the contract period.

To enhance the usability of the model for routine analyses, Phase I, currently in progress, involves the development of a graphical user-friendly interface which eliminates the need to master the underlying computer command language. The interface will provide the full capability to execute a model run and obtain results. It will also allow more expert users to easily modify the underlying models and algorithms -- a feature not available in most other models for power plant analysis.

Because of significant changes in technology status of many IECM components in recent years, Phase I also includes an extensive effort to upgrade and enhance many of the current technology modules in the IECM. In particular, efforts are focusing on the existing models for selective catalytic reduction (SCR), wet flue gas desulfurization (FGD), lime spray dryers, fabric filters, electrostatic precipitators, the NOXSO process and the copper oxide process. In each case, existing analytical models for the performance and cost of these technologies are being revised and upgraded to account for recent experience in the U.S. and elsewhere. In a companion task, all technology options currently embedded in the IECM are being extended to include a series of process retrofit factors that can account for the higher cost incurred when installing the new technology at an existing facility. The Phase I effort is scheduled for completion in September 1995.

Under Phase II, several new technology modules will be developed, along with linkages between the IECM and several existing PETC databases. The specific performance and economic models to be included in the Phase II research will be finalized later in the project, but may include such processes as advanced wet limestone FGD, duct injection technologies, sulfur recovery plants, reburning with coal or gas, cold-side SCR, the Tung process and slagging combustors. Additional personnel training, program debugging, and model documentation will be part of this effort, along with further enhancements of the graphical interface to accommodate the new technology modules.

During Phase II, linkages also will be developed with existing PETC databases to facilitate running the IECM for large numbers of cases. In particular, the PETC power plant database, the coal characteristics database, and the coal washability database will be linked to the model via a new interface capability to automatically read external files into the IECM. This work will be carried out in conjunction with PETC personnel responsible for the existing database. An automated interface with external data sets will allow the IECM to be used more extensively for market studies, technological risk evaluations, R&D management, and other special studies of interest to DOE.

PROJECT STATUS

As of May 1994, the project remains well on schedule, with several cost and performance model enhancements and upgrades already completed and documented. The new graphical interface to facilitate model operation also is nearing completion. Brief discussions of major project accomplishments over the past year appear below.

Performance and Cost Models

We have completed the development of new performance and cost models for all of the conventional technology components of the IECM, as well as a substantial enhancements to one advanced technology module for combined SO_2/NO_x removal. The new technology models to date include the following:

Flue Gas Desulfurization Systems. There have been substantial improvements in the performance of wet lime/limestone FGD systems in the past decade, coupled with design changes that have reduced capital and operating costs. The original IECM models for wet FGD systems were based on a detailed process model developed in the 1980s by the Tennessee Valley Authority (TVA). That model, however, is no longer maintained. The most recent updates to FGD economics were made by contractors for the Electric Power Research Institute (EPRI), who studies a large number of wet and dry FGD processes [10]. New algorithms for FGD capital and operating costs were derived from published EPRI studies and combined with new FGD performance models developed from survey information on current high-performance systems. Four types of wet and

dry FGD systems were modeled for the IECM: (1) wet limestone with forced oxidation to gypsum; (2) wet limetsone with dibasic acid additives; (3) wet-magnesium-enhanced lime; and (4) a lime spray dryer system.

Selective Catalytic Reduction Systems. As with FGD systems, SCR technology has seen significant cost and performance improvements in the past ten years. Recent studies based on operating experience on coal-fired power plants in Germany and Japan, plus detailed design studies for U.S. plants, provided the basis for updated performance and cost models for the IECM [11]. The new SCR models include: (1) hot-side systems located upstream of the air preheater, and (2) cold-side or tail-end systems located downstream of the FGD unit.

Particulate Removal Systems. Evolutionary changes to conventional cold-side electrostatic precipitators (ESPs) and fabric filters (baghouses) for coal-fired power plants also are reflected in new IECM performance and cost models. The new economic models are based primarily on recent studies for EPRI [12], while the revised performance models are based on other detailed modeling studies and empirical data for ESPs and fabric filters [13, 14].

Fluidized Bed Copper Oxide Process. This is one of three advanced processes for combined SO_2/NO_x removal incorporated in the IECM. Revisions to the original performance and cost models were based on new detailed design studies carried out for DOE [15].

Over the next year additional advanced process models in the IECM will be revised and updated based on the most recent studies and experience. Then, in Phase II, additional process models will be incorporated as discussed earlier. The resulting set of models will provide the most up-to-date basis for evaluating and comparing alternative coal-based power systems in a comprehensive and systematic fashion.

Graphical User Interface

As noted earlier, another major task of Phase I is to develop, implement and test a user-friendly graphical interface for the IECM. Work on this task will be completed by late 1994. Recent enhancements to the underlying model software environment have allowed us to create a flexible new interface design suitable for use by both novice and advanced model users.

For the novice user, the interface will allow a power plant design to be configured and analyzed for performance and cost, using either a deterministic or probabilistic format. For advanced model users, the interface also will facilitate the ability to examine and alter the underlying algorithms and equations that define the cost and performance of a given technology. This capability will allow researchers and DOE analysts to add new plant configurations or incorporate new data and design assumptions for specific components. Model results beyond those reported on standard output

screens also can be obtained in this fashion. This type of flexibility is not possible with other power plant models currently available.

REFERENCES

1. Rubin, E.S., *et al.*, *Modeling and Assessment of Advanced Processes for Integrated Environmental Control of Coal-Fired Power Plants.* Final Report of Contract No. DE-FG22-83PC60271 to U.S. Department of Energy, Pittsburgh, PA, July 1986, NTIS No. DE86014713/WEP.

2. Rubin, E.S., *et al.*, *Modeling of Integrated Environmental Control Systems for Coal-Fired Power Plants.* Final Report of Contract No. DE-AC22-87PC79864 to U.S. Department of Energy, Pittsburgh, PA, May 1991

3. Henrion, M. and N. Wishbow. *Demos User's Manual: Version Three.* Carnegie Mellon University, Department of Engineering and Public Policy, Pittsburgh, PA, August 1987.

4. Rubin, E.S., J.S. Salmento and H.C. Frey. "Cost-Effective Emission Control for Coal-Fired Power Plants," *Chemical Engineering Communications*, 74 (1988), 155-167.

5. Frey, H.C., and E.S. Rubin, "Probabilistic Evaluation of Advanced SO_2/NO_x Control Technology," *Journal of the Air and Waste Management Association*, 41(12):1585-1593 (December 1991).

6. Frey, H.C., and E.S. Rubin, "An Evaluation Method for Advanced Acid Rain Compliance Technology," *Journal of Energy Engineering*, 118(1):38-55 (April 1992).

7. Frey, H.C., *Probabilistic Modeling of Innovative Clean Coal Technologies: Implications for Research Planning and Technology Evaluation,* Ph.D. Thesis, Department of Engineering and Public Policy, Carnegie Mellon University, Pittsburgh, Pennsylvania, May 1991.

8. Salmento, J.S., M.B. Berkenpas, S.A. Siegel, *Technical Manual for the Integrated Environmental Control Model,* Report of Contract No. DE-AC22-87PC79864 to U.S. Department of Energy, Pittsburgh, PA, August 1991.

9. Rubin, E.S., et al. "Development of the Integrated Environmental Control Model," Quarterly Report to the U.S. Department of Energy, Contract No. DE-AC22-92PC91346, from Carnegie Mellon University, Pittsburgh, PA, January 1993.

10. Keeth, R.J., Baker, D.L., Tracy, P.E., Ogden, G.E., Ireland, P.H., "Economic Evaluation of Flue Gas Desulfurization Systems," *Report No. GS-7193,* Electric Power Research Institute, Palo Alto, CA (1991).

11. Frey, H.C. and E.S. Rubin, "Development of the Integrated Environmental Control Model: Cost Models of Selective Catalytic Reduction (SCR) NO_x Control Systems," Quarterly Progress Report to Pittsburgh Energy Technology Center, Contract No. DE-AC22-92PC91346-5, from Center for Energy and Environmental Studies, Carnegie Mellon University, Pittsburgh, PA (January 1994).

12. Sloat, D.G., Gaikwad, R.P., and Chang, R.L., "The Potential of Pulse-Jet Baghouse, Precipitators, and Reverse Gas Baghouses," *Journal of Air and Waste Management Association,* Vol. 43, pp. 120 (1993).

13. Bickelhaupt, R.E., "Fly Ash Resistivity Prediction Improvement with Emphasis on Sulfur Trioxide," EPA-600/7-86-010, Environmental Protection Agency, Washington, DC (1986).

14. Electrostatic Precipitators vs. Fabric Filters: A Symposium and Debate, *Institute of Clean Air Companies,* Washington, DC (1994).

15. Frey, H.C., *Modeling and Assessment of the Fluidized Bed Copper Oxide Process for SO_2/NO_x Control,* prepared for U.S. Department of Energy by North Carolina State University, Raleigh, NC, March 1994.

CERAMIC FILTER FOR FINE PARTICULATE CONTROL

BRUCE A. BISHOP, RICHARD F. ABRAMS, AND ROBERT L. GOLDSMITH
CERAMEM CORPORATION
12 CLEMATIS AVENUE
WALTHAM, MA 02154

Abstract

A novel, high efficiency, compact ceramic filter has been developed for particulate removal from flue gas and hot gas streams. These filters were tested in a 5,000 ACFM, 1.5 MW flue gas pilot plant. Due to filter fouling by a thin layer of cementitious ash, the initial filter pressure drop after backpulse cleaning could not be completely recovered. Based on experimental results from other successful filtration runs and a steady state gas flow pressure drop analysis, it was determined that parasitic pressure losses due to flow down the small, 12" long filter passageways minimized the efficiency of the gas backpulses in removing deposited ash layers. Preliminary results on an incinerator application have indicated that minimizing the channel flow pressure drop in the filters leads to effective filter regeneration.

Description of Filter

The gas particulate filter developed in this program is based on a porous honeycomb ceramic monolith. These monoliths are available commercially from Corning, Inc. The honeycombs used to produce the ceramic filters are made from a cordierite material which has about 50% porosity and an average pore size between 12 and 35 μm. The monoliths used to date are typically 5" to 9" across (both round and square cross sections) and 6" to 15" long. The monoliths have a multiplicity of "cells" (passageways) which extend from an inlet end face to an opposing outlet end face. The filter cell geometry is square and the cell "density" is typically 25 (0.17" channel height) or 100 (0.08" channel height) cells per square inch of frontal area.

CeraMem uses the porous monolith supports to fabricate filters by first coating the passageways with a porous ceramic membrane layer and then plugging appropriate inlet and outlet passageways. The membrane layer is cast by filling the passageways with a liquid medium ("slip") containing a mixture of ceramic powders and organic additives. The pore structure of the monolith walls absorbs water from the slip, forming a cake of particles on the wall surfaces at the slip/wall interface, then the coated monolith is dried and fired to 1100+°C to bond the ceramic membrane particles to themselves and the monolith. After coating, every other cell at the upstream face of the device is plugged with a high-temperature inorganic cement and the cells which are open at the upstream face of the monolith are plugged at the downstream face.

A particulate laden gas stream entering the filter is constrained to flow into an inlet passageway at one end face, through the membrane coated wall, and then out one of the adjacent outlet passageways. The fine pored membrane (ca. 0.5 μm) is thin compared to the coarse pored monolith walls adding the minimum amount of gas flow pressure drop necessary to create a high efficiency particulate filter. The particulates retained by the filter are trapped at the membrane surface and do not enter the monolith pore structure. This allows the particulates to be removed by gas backpulsing at regular intervals after the filter passageways have been significantly filled with ash and the pressure drop has increased.

Ceramic filters in a variety of configurations are currently being produced by CeraMem. Some of these are described in Table I. The compactness of the filters relative to other flue gas filters is evident from the comparative data in Table I. This leads to very compact systems which are expected to have lower costs than traditional flue gas particulate filtration systems, arising from a substantial reduction in the size of the housing and installation costs.

TABLE I

EXAMPLES OF CERAMIC FILTERS: SIZES AND FILTRATION AREA

Cross Section	Size	Length	Cell Density	Filter Area
Round	5.66" dia.	6"	100 cpsi	10 ft^2
Square	5.9" side	12"	100 cpsi	37 ft^2
Square	5.9" side	12"	25 cpsi	18 ft^2

COMPARISON OF CERAMIC FILTERS WITH FABRIC FILTERS

Filter Type	Filter Dimensions	Area/Volume Ratio
Ceramic Filter	5.9"x5.9"x12"; 100 cpsi	155 ft^2/ft^3
Ceramic Filter	5.9"x5.9"x12"; 25 cpsi	75 ft^2/ft^3
Fabric Bag Filter	12" diameter	4 ft^2/ft^3
Fabric Bag Filter	6" diameter	8 ft^2/ft^3

Individual Filter Tests

Tests of individual filters for fine particulate removal have been conducted at 18 sites as of February, 1994. The duration of the tests has ranged from 48-1100 hours at gas flow rates from 20-600 ACFM. These tests, summarized in Table II, have been very successful and have generated several conclusions which are stated below:

1. Filtration face velocity (equivalent to an "air to cloth ratio") is comparable to that for pulse jet bags at the same pressure drop.

2. Complete regeneration by a simple backpulse technique can be achieved; i.e., no increase in clean filter resistance over repetitive cycles.

3. No plugging of the filter passageways is observed under normal operating conditions even with badly caking particulate matter.

4. Complete particulate removal (effluent particulate concentrations lower than the limits of detection), including submicron particulate matter, is achieved.

Review of Pilot Plant Demonstration

In March and April of 1993, CeraMem conducted initial filtration tests on a 5,000 ACFM, 1.5 MW flue gas pilot plant at the Public Services of Colorado's Comanche Station. Comanche is

a coal-fired power plant burning Powder River Basin sub-bituminous coal. The pilot plant, described previously[1], contained 36 filters which were 5.9" in cross section and 12" long with a cell density of 100 cpsi. The total filter area installed into the system was about 1332 ft^2. For initial start-up, clean, hot flue gas was introduced to the system to check filter pressure drop and system controls. All controls checked out well, and the filter array pressure drop was about 6" WC at 4 ft/min face velocity.

TABLE II. FIELD TESTS OF INDIVIDUAL CERAMEM FILTERS

Test Site	Application	Temp.	Pressure
Gulf Power, Plant Scholz	Atm. Coal Comb.	250°F	atm
Exxon Research & Eng.	Coal Comb.	300°F	atm
MHD Facility	Sorbent/Ash	300°F	atm
Berkshire Medical Center	Med. Waste Incin.	300°F	atm
Northeastern University	Diesel Filtration	450°F	atm
Private Company	Gasification	500°F	300 psi
Private Company	Diesel Filtration	500°F	atm
Fiberglass Boat Manuf.	VOC/particulate	550°F	atm
ADL/MIT	NO_x/SO_2/particulate	700°F	atm
Private Company	Flue Gas/NO_x	750°F	atm
Exxon Research and Eng.	NO_x/particulate	750°F	atm
Private Company	Ceramics Manuf.	1000°F	10 psi
Exxon Research and Eng.	Sorbent/Ash	1000°F	atm
Westinghouse	PFBC Hot Gas	1200°F	100 psi
Univ. of North Dakota	Coal Gasification	1200°F	10 psi
CeraMem/MIT	H_2S sorbent	1400°F	atm
Westinghouse	PFBC Hot Gas	1600°F	150 psi
Alhstrom	PFBC Hot Gas	1800°F	300 psi

After the system was checked out, particulate-laden flue gas was introduced to the system. Over the first few filtration cycles, the clean filter pressure drop could not be recovered via backpulse cleaning at pressures up to 95 psig with multiple pulses. Subsequent tests of various backpulse conditions, including cleaning the filters with no inlet flue gas flow (i.e., off-line), made no significant difference to the filter pressure drop. The system was shut down and the filters inspected in the field for passageway plugging. No plugged cells were detected. Compressed gas at 40 psig was used to clean the filters by hand. Significant amounts of ash were observed to come out of the filters but no change in filter pressure drop was found. As a result of these tests, one row of four filters was removed and sent back to CeraMem for analysis.

One of the filter elements taken from the Comanche pilot plant was analyzed by measuring gas flow pressure drop before and after several cleaning operations. Table III summarizes the cleaning analysis of the filter. The dirty filter pressure drop was decreased with manual pressurized gas backpulse cleaning. Overall, about 0.5 pounds of ash were removed from the module. However, aggressive backpulse cleaning was not sufficient to completely recover the clean filter pressure drop. The filter was then exposed to a series of aqueous cleaning cycles. Washing with water and an aqueous detergent solution were effective in reducing the filter pressure drop and seemed to loosen up the ash so that it could be removed by backpulsing.

Even though the pressure drop was significantly reduced, only a small amount of ash was removed with water washing indicating that the ash layer being removed had a very low permeability. The final filter pressure drop after the intense cleaning, measured at room temperature, was only slightly higher than the original clean filter pressure drop.

Small pieces of the filter were extracted at various times in the cleaning analysis for examination by scanning electron microscopy (SEM). Observation of the membrane surface showed that the surface was coated with a thin, dense layer of ash that could not be removed by gas backpulsing and could not be completely removed by water washing. Also, the primary ash particles appeared to be cemented together by small, sub-micron particles or needle-like crystals consistent in morphology with that of gypsum ($CaSO_4 \cdot 2H_2O$).

TABLE III. SUMMARY OF GAS FILTER CLEANING ANALYSIS

Cleaning Process	Resultant dP @ 4 ft/min	Filter Wgt after Cleaning
Clean filter pressure drop	4-5" WC	---
Received from Comanche	10" WC	9.90 lbs
Reverse air flow, low dP	10" WC	---
Clean cells with 70-100 psi gas	9" WC	9.60 lbs
Clean cells with 100 psi gas until no additional dust is removed from filter	7.25" WC	9.40 lbs
Flush with water, dry overnight	6" WC	9.35 lbs
Soak in detergent solution, flush, dry	5.5" WC	9.35 lbs
Clean cells with 100 psig gas	5.2" WC	9.35 lbs

These observations in combination with the cleaning analysis, led to the conclusion that a thin, dense layer of cementitious ash was adhering to the membrane surface making it difficult to clean the filter by pressurized gas backpulsing. It was hypothesized that the backpulse gas was cooling the flue gas resulting in moisture condensation. This moisture, interacting with the high calcium ash, may have cemented the ash layer to the membrane. As a result, the pilot plant was modified to incorporate a hot gas backpulse system.

After designing and procuring the equipment, the hot gas backpulse system was installed in the pilot plant in October, 1993. In addition, new filters were manufactured for the restart and some modifications of the dirty side gas baffle system were made in order to minimize particulate reintrainment during backpulsing. As before, the system was started on clean, hot flue gas to check system controls and filter gas flow pressure drop. All systems checked out well, including the hot gas backpulse system which could generate gas in sufficient quantities at 100 psig and 400°F for backpulsing. The second set of filters had the same gas flow pressure drop characteristics as the first set.

After system check-out on clean flue gas, hot particulate-laden flue gas was introduced to the pilot plant. The filters were operated starting at 3.7" WC clean filter pressure differential at 2.4 ft/min face velocity. Initial off-line backpulse cleaning of the filters using 400°F air at 100 psig was performed in three, 0.4 second pulses per filter after the filter array reached 5" WC.

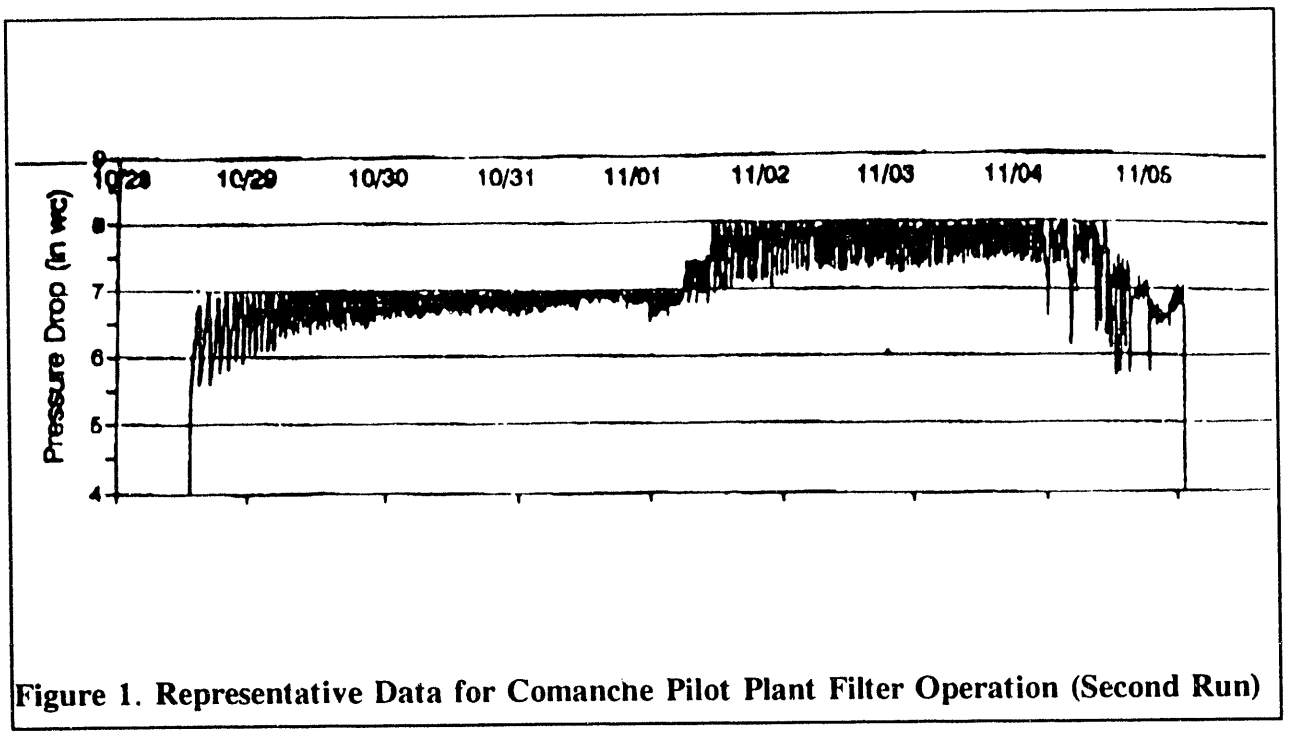

Figure 1. Representative Data for Comanche Pilot Plant Filter Operation (Second Run)

The system was operated to determine the effect of the system changes. As shown in the representative data in Figure 1, the clean filter pressure drop increased over time. The cleaning set point was increased from 5" WC to 8" WC over several steps. After each increase in the cleaning set point, the clean filter pressure drop would slowly increase and approach that of the set point. As the set point was raised, the rate of increase in clean filter pressure drop did appear to slow down. In all, about 430 hours of system operation were logged until the power plant experienced technical difficulties and had to shut down.

Pilot plant system changes may have improved the filter regeneration, but the filters were still not cleaning well. Even if the filters were run longer to determine if the filter cleaning would have stabilized at 8" WC, the filter drag (pressure drop in inches of water/face velocity in feet per minute) would have been about 3. Although the initial filtration drag parameter of the system was commercially viable, filter fouling with time increased drag to an unacceptable level.

Interpretation of Comanche Results

The increase in pressure drop across the gas filters appears to be due to the build up of a very thin layer (dustcake) of fine fly ash particles on the filter surfaces. It is relevant that this behavior has not been observed in about 20 field trials with 6" long filters, in contrast to the 12" long filters used at Comanche and two other sites at which dustcake layer build up has been observed. Consequently, CeraMem has performed an analysis of the relative resistances to steady state flow through the gas filters to determine the effect of length on gas backpulsing.

CeraMem evaluated the components of the gas filter flow resistances which are due to the passageways, membrane, and monolith wall. Using dimensions of typical gas filters, room temperature gas flow pressure drop data on membrane-coated and non-membrane-coated filters, and the engineering relationships between flow and pressure drop for both laminar and turbulent flow, the plots in Figures 2 and 3 were calculated.

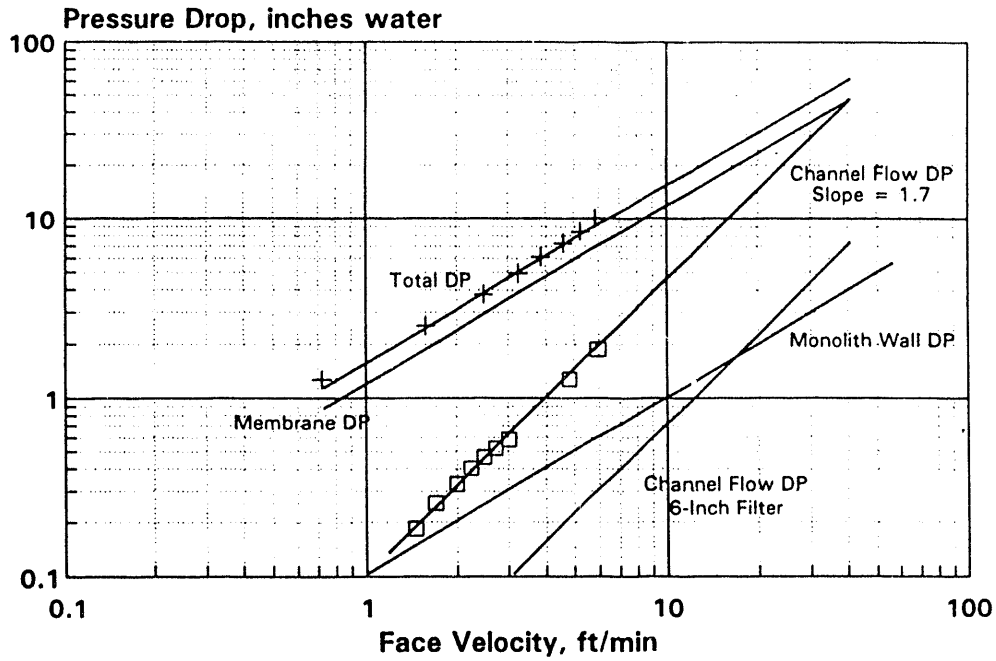

Figure 2. Total & Component Gas Flow Pressure Drops for a 100 cpsi, 12" Long Filter

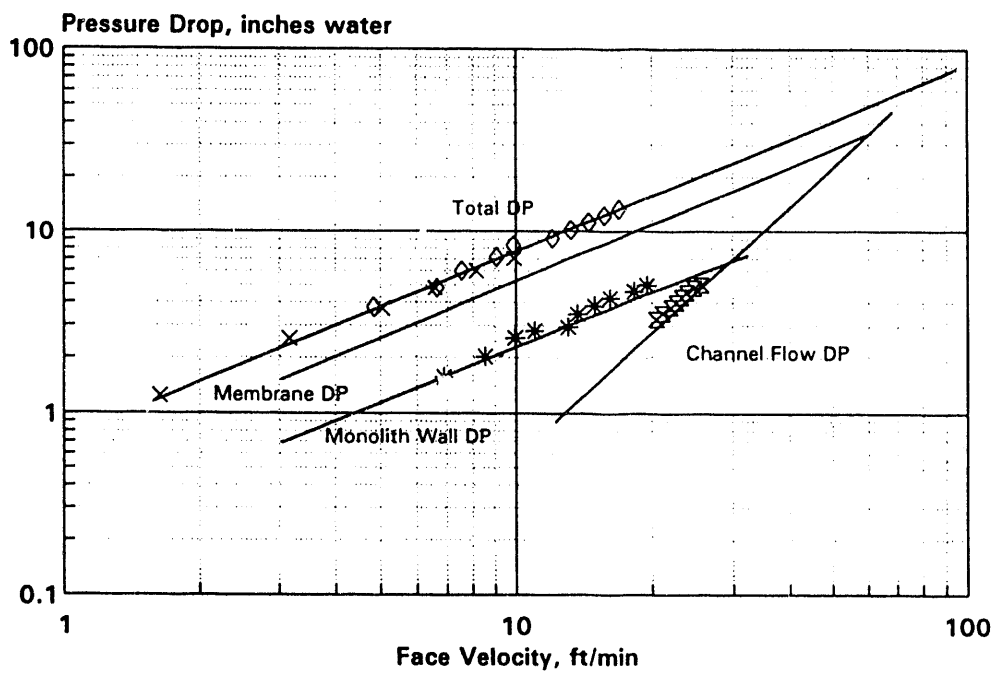

Figure 3. Total & Component Gas Flow Pressure Drops for a 25 cpsi, 12" Long Filter

Figure 2 shows the approximate gas flow pressure drop of a 12" long, 100 cpsi membrane coated filter at 300°F (Total DP) and each of the component pressure drops (Membrane DP, Channel Flow DP, Monolith Wall DP). In addition, the effect of shortening the filter to 6 inches on the channel flow pressure drop is included. It can be seen that the membrane pressure drop is the dominant resistance at normal operating conditions (4"-6" WC) . However, during backpulse cleaning the pressure drop can be about 2 psi (52" WC). Under these conditions, the channel flow pressure drop for a 12" filter becomes the same as, if not higher than, the membrane pressure drop. Consequently, the ash layer will be exposed to limited backpulse pressure due to parasitic pressure drop losses. If the filter was only 6" long, then the channel flow pressure drop would be considerably reduced and more of the backpulse pressure would be directed across the ash layer. This may explain why 6" long filters have been regenerable by pressurized gas backpulsing and 12" long filters have been much more difficult to regenerate.

Figure 3 shows the approximate gas flow pressure drop of a 12" long, 25 cpsi membrane coated filter at 300°F and each of the component pressure drops. It is apparent that the channel flow pressure drop is significantly lower for the 25 cpsi filter (7" WC at 30 ft/min) than the 100 cpsi filter (30" WC at 30 ft/min). This is due to the increased cell size (0.17" versus 0.08"), since the decrease in channel flow pressure drop varies with the square of the cell size. As with the 6" filter, the decreased channel flow pressure drop will increase the amount of pressure differential across the ash layer thereby increasing the probability that the ash will be removed.

Comparison of 100 cpsi and 25 cpsi Filters

Based on the analysis briefly described above, two different filters have been tested on a 300-350°F flue gas from an incinerator application. First, a 100 cpsi, 12" long filter was installed in a single filter housing equipped with an automatic backpulse system. The system was installed on a slipstream in parallel with a fabric filter baghouse running on a medical waste incinerator which is known to contain a substantial quantity of sub-micron particles in the flue gas. The filter was run for one day over which the initial filter drag could not be recovered by two backpulse cleanings. It appeared that the filter, which was similar to that used for Comanche, would not operate well in this application.

A second filter with 25 cpsi and 12" length was installed in the filtration system. The filter has been operated for more than 300 hours. The filter drag over this time period appeared to be stable within the variation of the incinerator operating conditions. This filter will be removed and analyzed before any firm conclusions will be drawn; however, the filter seems to be regenerable by pressurized gas backpulsing.

Summary

A novel ceramic filter has been developed with high particle removal efficiency, ability to be cleaned by backpulsing with compressed air, and very high surface area per unit volume. Thirty-six filters were installed in a 5,000 ACFM pilot plant at Public Services of Colorado's Comanche Station. Two attempts were made to operate the filters on ash-laden flue gas but due to filter fouling by the fly ash, the clean filter pressure drop could not be maintained. Based on the observation that 100 cpsi, 6" long filters were regenerable and that 12" filters with similar passageway size were not, CeraMem conducted an analysis of the resistances to gas flow for these filters. The conclusion was that parasitic pressure losses during backpulse cleaning due, at least in part, to gas flow down the filter passageways may limit the pressure differential across the ash layer which may lead to ineffective cleaning. Subsequent testing on a medical waste

incinerator indicated that filters with lower channel flow pressure drops may be fully regenerated via pressurized gas backpulse cleaning.

Additional testing is necessary to understand the mechanisms involved in cleaning these novel filters. CeraMem plans on continuing its testing of various filters in the incinerator application. CeraMem is also planning on testing its filters at Alabama Power's Plant Miller Station on a COHPAC application in conjunction with EPRI as well as restarting the Comanche pilot plant with new filters in 1994. Additional computer modelling of filter operation, especially backpulse cleaning, will be conducted in 1994 and used to help interpret experimental results.

Acknowledgments

The development effort for the filter was supported by the DOE under a Phase II SBIR Grant (No. DE-FG-02-90ER80897). Mr. Thomas D. Brown of the Pittsburgh Energy Technology Center is the Project Officer. Also, the development of this technology is being assisted by EPRI, the Electric Power Research Institute, under Technology License Agreement RP1402-61.

References

1. Goldsmith, R.L. and Abrams, R.F., "Ceramic Filter For Fine Particulate Control," Proceedings of the Ninth Annual Coal Preparation, Utilization, and Environmental Control Contractors Conference. July 19-22, 1993. DOE-PETC. pp. 539-546.

EVALUATION AND FURTHER DEVELOPMENT OF VARIOUS SAMPLING AND ANALYTICAL METHODS FOR DETERMINING SPECIFIC TOXIC EMISSIONS FROM COAL-FIRED POWER PLANTS

R. P. KHOSAH, J. CLEMENTS, R. O. AGBEDE
ADVANCED TECHNOLOGY SYSTEMS, INC.
SUITE 201, 339 HAYMAKER ROAD
MONROEVILLE, PA 15146

SUMMARY

A literature search of the state-of-the-art sampling and analytical methodology for size-fractionated particulate and vapor phase samples from stack effluents was performed. The identified methodology was compared with that employed by the five contractors that the Department of Energy (DOE) selected to conduct a series of air toxic emission tests at nine test sites. In addition, a critique of the emission studies reports generated by the five contractors were performed based on several test/target criteria. These criteria included data quality and integrity, adherence to QA/QC protocol, satisfaction of DOE objectives from the findings, and the identification of opportunities for method improvements.

[Complete paper will be available at the meeting.]

The following manuscript was unavailable at the time of publication.

OXIDE-BASED CERAMIC COMPOSITE HOT GAS FILTER DEVELOPMENT

E. L. Paquette
Ceramic Composites, Incorporated
1110 Bentfield Blvd.
Millersville, MD 21108

Please contact author(s) for a copy of this paper.

The following manuscript was unavailable at the time of publication.

INNOVATIVE SiC FIBER COMPOSITE FILTERS

R. O. Loutfy
Materials and Electrochemical Research Corporation
7960 S. Kolb
Tuscon, AZ 85706

Please contact author(s) for a copy of this paper.

PLASMA-ASSISTED NH_3 INJECTION FOR NO_X CONTROL

by

Karen Chess
Professor Shi-Chune Yao
Professor Armistead Russell

Department of Mechanical Engineering
Carnegie Mellon University
Pittsburgh, Pennsylvania 15213-3890

The control of NO_X emissions from many utility boilers is required under the acid rain provisions of the 1990 Clean Air Act Amendments. While these provisions specify reduced emission factors achievable with combustion modifications, additional emission reductions may be necessary to comply with Title I of the Act to control ground-level ozone in some areas (e.g., Possiel, 1991). Such additional requirements would potentially be met with post-combustion, flue gas treatment controls like selective non-catalytic reduction (SNCR) and selective catalytic reduction (SCR).

SCR and SNCR both use chemical reactions with ammonia (NH_3) or other agents to reduce the amount of NO_X emitted into the atmosphere. SNCR processes, such as Thermal $DeNO_X$® (Lyon, 1975), inject cold NH_3 into combustion flue gases and rely on a narrow temperature window of 1100-1370 K (Salimian and Hanson, 1980) to dissociate the NH_3 for subsequent reduction reactions. SNCR generally achieves 40-60% NOx reduction in commercial applications. In contrast, SCR can achieve 80-90% NO_X reduction by introducing a catalyst grid into the ammonia injection process to aid dissociation (EPA, 1992a). However, the introduction of the catalyst increases the expense of the reduction process considerably (EPA, 1992b).

In an effort to lessen the dependence on a temperature window and to avoid the expense of a catalyst, a new approach using plasma technology was developed for NO_X reduction. In it, ammonia radicals were created with plasma generators and injected into combustion flue gases. By breaking down the NH_3 externally, the reliance on the temperature window and catalyst were avoided. Two independent studies, one on a laboratory-scale combustor (Zhou, et.al., 1992) and the other on a larger test facility (Boyle, et. al., 1993), demonstrated the potential of ammonia radical injection to achieve high NO_X reduction. Zhou et. al. at Carnegie Mellon found a maximum NO_X reduction of 86% using an inductively coupled plasma system (ICP-16), while Boyle et. al. found 85-90% NO_X reduction at PETC using a DC plasma torch. Both experimenters found that NO_X reduction increased with increased ammonia flow, decreased plasma power, and decreased excess air.

While the radical injection technique for NO_X control shows promise, several key questions remain concerning its performance and its place relative to other post-combustion control techniques. For example, since the radicals in this process are necessarily injected at elevated temperature, the high level of NO_X reduction achieved could be the result of increased NH_3 dissociation by thermal breakdown within the combustor as well as the result of the presence of externally produced radicals. These two effects, bulk thermal heating and radical production via interaction with the plasma, must be separated in order to determine if the application of plasma technology to NO_X control is the means by which the high NO_X reduction was achieved in the demonstration experiments. Once this plasma effect is verified, further experiments designed to explore the fundamentals of the plasma process for NOx control will be necessary to gather information to scale up and optimize the process for commercial application.

This paper presents the results of an experiment designed to distinguish the thermal effect from the radical (or plasma) effect in the plasma-assisted ammonia injection process for NO_x control, and it introduces a new experiment under construction that will be used to explore the process on a more fundamental level. In the completed experiment, the lab-scale apparatus used in previous demonstrations of the process was modified by replacing the plasma system for ammonia radical injection with a system to inject hot NH_3 and a carrier gas. In this way, NO_x reduction by the thermal effect was allowed, but NO_x reduction by the radical effect was prevented, such that the two effects could be separated and quantified. In the new experiment, opposing jets of plasma gas and combustion flue gas will be constructed and used in conjunction with an analytical model of the system to gain insight into the process fundamentals.

Hot Injection Experiment

Design

To isolate the thermal effect from the radical effect in the plasma-assisted ammonia injection process for NO_x control, an experiment using hot NH_3 injection was designed to mimic conditions in previous work by Zhou et. al.. The relative NO_x reduction advantage of hot NH_3 to cold NH_3 injection, a measure of the thermal effect, was investigated directly. The advantage of plasma injection over hot NH_3, a measure of the radical effect, was inferred by duplicating conditions from the previous work, using hot injection instead of the plasma system. Figure 1 shows the overall apparatus used in Zhou's plasma experiments and in the hot injection investigations. The combustor and the fuel injector measured 15 cm and 1 cm in diameter, respectively, and the length of the combustion chamber was 150 cm. A methane diffusion flame was doped with nitric oxide (NO) to raise the NO concentration in the combustor for study. The ammonia, carrier gas, and combustion gas flow rates used in the plasma and hot injection experiments were identical. NO and NO_x concentration measurements were made with a Thermo-Electron 10AR chemi-luminescent NO/NO_x analyzer. Gas flow measurements were made with rotameters, and temperatures were measured with Chromel-Alumel (Type K) thermocouples.

The plasma gun system used in the radical injection process is described by Zhou et al.. In the hot injection study, this system was replaced with an apparatus for heating and injecting hot ammonia and argon (as the carrier gas) into the combustor, as shown in Figure 2. Argon was passed through a 100 cm stainless steel tube whose temperature was controlled by varying the DC current supplied to the tube for direct Joule heating. The hot argon gas then passed into an injector designed to mimic the geometry, and therefore the swirling flow conditions, of the plasma gun. Cold NH_3 was introduced tangentially into the injector, where it mixed with the hot argon gas before being injected into the combustor. The injector was positioned approximately 8 cm from the combustor, as was the plasma gun in the previous experiments. An electrically insulated nozzle connecting the injector to the combustor minimized the amount of ambient air entrained by the hot jet. In the plasma experiments, a larger guard box produced a similar effect. Finally, the entire hot tube and injector were insulated to minimize heat loss.

The achievable temperatures of the gas exiting the hot tube apparatus were dictated by the limitations of the materials used. At peak operating conditions, the hot tube reached 1150 K with 740 W supplied by the electrical source. Only a portion of this power was actually used to heat the injected gases, with the remainder being lost thermally and radiatively. It was of concern whether the power input to the injection gases in the hot tube experiments was similar to the power input to the injection gases in the plasma experiments. In the subset of data selected from the plasma experiments for comparison, the power supplied to the plasma gun was 400 W. However, this power included losses through the cooling system, EMF losses, and others. At peak power in the hot tube experiments, the argon/ammonia stream entered the combustor at about 850 K. Based on this temperature and a mean specific heat and density of argon, the power actually carried into the

combustor by the input gases was about 215 W. In the plasma experiments, the temperature at the injection section was reported as 920 K (Zhou, 1991), which would correspond to a power input of about 240 W. Thus, the power supplied to the injected gases in both experiments was comparable.

Results

Throughout the experiments, little or no difference was detected between the NO and NO_x measurements, which is consistent with commercial measurements indicating that 90% or more of NO_x emissions from utility boilers is NO. Since the combustion gases in the present experiments were doped with NO, emission reductions are reported as the percent NO reduction relative to a baseline of no ammonia injection. In reporting NO reduction performance, "flue gas temperature" is the temperature of the combustion flue gas at the centerline of the combustor, as measured approximately 5 cm below the ammonia injection port.

Figure 3 shows typical results for NO reduction with cold and hot NH_3 injection over a range of combustor temperatures at 25% excess air conditions similar to those in the high reduction plasma experiments. As shown, hot NH_3 injection was moderately more effective than cold injection at all flue gas temperatures investigated, and NO reduction increased with combustion temperature. The difference between the two curves in Figure 3 is an indication of the thermal benefit of heating the ammonia before injection at these conditions.

To capture the actual benefit of generating ammonia radicals for injection using plasma technology, data from the previous plasma experiments were compared to hot injection data obtained under similar combustion and ammonia flow conditions. The plasma experiments by Zhou were not used to explore the effect of flue gas temperature on NO_x reduction, so the data relevant to such a comparison with hot ammonia injection are sparse. Multiple data points for NO_x reduction at the same excess air condition but different combustion temperatures were found for 0% excess air only. Figure 4 shows results for NO reduction at 0% excess air plotted against combustion flue gas temperature. The combustion temperature was not reported in the plasma experiments, and so it is assumed that the temperatures found in the hot injection experiments at the same fuel and air conditions apply. This is consistent with reports by Zhou that the plasma injection process did not affect the temperature below the injection point. The difference between the two curves in Figure 4 indicates that there is a benefit to externally generating ammonia radicals that is due to the presence of the radicals themselves and is beyond the thermal benefit of hot injection.

While the lack of plasma experiment data precluded making further comparisons between plasma and hot ammonia injection over a range of flue gas temperatures holding other conditions constant, direct point comparisons between the two sets of data give insight into the NO_x reduction effectiveness of each under identical conditions. In this way, the relative contributions of thermal and plasma effects can be clearly seen in Figure 5. The plasma experiment data provided four points in which all conditions were held constant except for the air flow rate. These conditions were duplicated using both hot and cold injection, leading to direct point comparisons among hot NH_3, cold NH_3, and radical injection at four excess air conditions. Since the combustion temperature increased with decreasing excess air (the same amount of fuel was used in all four cases), the difference between the NO reduction values in the columns in Figure 5 include two separate effects. However, between the 0% and 25% excess air conditions, which is a typical range for commercial boilers, the flue gas temperature increase was no more than 16 K, indicating that the excess air condition itself was the dominant variable. The average combustion temperatures at 75%, 50%, 25%, and 0% excess air were 922 K, 938 K, 960 K, and 976 K, respectively. The data for hot, cold, and radical injection in each column in Figure 5 were obtained for identical gas flow conditions. For each condition, the fraction of the total NO reduction attributable to each effect is indicated by the relative sizes of the shaded sub-regions compared to

the overall column height. As shown, NH_3 injection was more effective at lower levels of excess air. The effect of heating the NH_3 before injection was negligible at 50% and 75% excess air, but became significant at 25% excess air and more so at 0%. In contrast, the contribution of the use of the plasma generator to NO reduction was largest at the higher levels of excess air. This plasma effect contribution was offset by the thermal effect at lower amounts of excess air, but was still significant in all cases.

Discussion

The hot injection experiment was designed to verify that the high NO_x reduction achieved in the two demonstration studies of plasma-assisted ammonia radical injection was not due merely to the bulk thermal heating of the ammonia stream by the plasma systems used. The results show that this thermal effect is significant in some cases, particularly at lower levels of excess air, but it does not account for the high NO_x reductions achieved in the plasma process demonstrations. The advantage of externally generating the ammonia radicals via interaction with the plasma was significant at all conditions tested. At excess air conditions between 0-25%, typical of utility and industrial boilers, the plasma effect accounted for 15-35% additional NO_x reduction beyond any thermal benefit.

Since the advantage of the plasma process has been verified with data from the hot injection experiment and the lab-scale demonstration project, further research is warranted. The demonstration projects identified several of the major factors affecting NO_x reduction performance, including ammonia and carrier gas flow rates, excess air conditions, and plasma power. However, these projects were narrow in scope in the sense that the potential of the plasma process to reduce other pollutants and to perform well using alternative reagent and carrier gas combinations over a wide range of operating conditions remains largely unexplored. In addition, the investigations in the demonstration projects were undertaken from a global perspective, exploring the effect varying the factors had on overall NO_x reduction without being concerned with the more fundamental mechanisms associated with the process.

Preliminary work by Boyle et. al. did study the basic chemical reactions that might lead to the NO_x reductions observed, and concluded that amidogen (NH_2) was the primary reducing agent according to the following reaction:

$$NH_2 + NO \Rightarrow N_2 + H_2O \qquad (1)$$

However, the chemical kinetics model used assumed a homogeneous mixture, which limits the information gained to identifying dominant chemical reactions and overall temperature effects. To scale the plasma process up to practical applications and to optimize its performance, more detailed information is required.

Opposed Jet Experiment

The plasma injection process is diffusional in nature, involving the mixing of the radical gas stream with the combustion flue gas. At the interface of these two streams, the NO_x reduction reactions occur. Because the interface is turbulent and the reactions are at non-equilibrium, the study of the fundamentals of the plasma injection process for NO_x reduction is difficult. To study the fundamentals of plasma injection at conditions relevant to the turbulent mixing process, an experiment using opposing laminar jets of plasma gas and combustion exhaust has been designed. The laminar opposed jet reaction system serves as a model for simulating the laminar eddy reactions in turbulent mixing layers. In addition, this system can be used to quickly investigate alternative process gas combinations at a wider range of operating conditions.

The main apparatus of the opposed jet experiment currently under construction is shown in cross-section in Figure 6. The inductively coupled plasma gun used by Zhou provides the lower jet of ammonia radicals and carrier gas, while a small methane burner provides combustion gases for the upper jet. Where the two jets meet, a stagnation plane is formed. NO gas will be bled into the combustion gases at the centerline of the upper jet, so that high NO concentrations for study will follow the stagnation plane. Temperature and NO_x concentration data will be taken in the vicinity of this plane and, coupled with a numerical analysis of the opposed jet system, insight into the NO_x reduction mechanism will be gained.

Laminar opposed jet systems have been used extensively in the past to investigate fundamental processes in turbulent diffusion flames (e.g., Potter, et.al. (1959), Hahn, et.al. (1981), Miller, et.al. (1992)). As such, the fluid mechanics, heat transfer, and mass diffusion in these systems is well known. The numerical analysis of the current system will capitalize on this work while paying attention to differences between the past and proposed systems. For example, analysis of the current system will not involve the high temperature gradients associated with the diffusion flame experiments. In solving the opposed jet system, the fluid mechanics will have a known solution and the temperature and species profiles will be simulated. Reactions will likely be simulated with CHEMK, a chemical kinetics solver (Whitten and Hogo, 1980).

The opposed jet system will also be used for further exploratory projects investigating NO_x and SO_x reduction using alternative reagent and carrier gases. Other choices of reagent might include methane (CH_4), which is used in the reburn process for NO_x control, as well as acetylene (C_2H_2) or urea. Reagent combinations are also possible. Potential carrier gases include nitrogen, steam, or combustion products such as flue gas. The use of alternative gases in the radical injection process may lead to increased NO_x reduction over a wider range of operating conditions and to a reduced cost effectiveness ($/ton of pollutant removed) of the process.

Summary

Current research into the plasma-assisted radical injection process for NO_x control focuses on verifying the advantage of externally generating the ammonia radicals via interaction with the plasma and on exploring the mechanism of NO_x control on a more fundamental level. Results of the hot injection experiment showed that the high NO_x reduction achieved in previous demonstrations of the plasma process could not be explained by the bulk thermal heating of the injected ammonia and carrier gases. Thus, the advantage of externally producing ammonia radicals has been confirmed. To explore the plasma process fundamentals and alternative process configurations, an opposed jet system has been designed to simulate the laminar eddy reactions associated with the turbulent diffusional nature of the injection process.

The plasma-assisted radical injection process for NO_x control continues to show promise as a control technique capable of SCR-typical NO_x reduction without the reliance on a narrow temperature window or catalyst to dissociate the ammonia or other reagent. Past demonstrations of the process have been exploratory and global in nature. As the more fundamental mechanisms in the plasma process are studied and as alternative process gases and operating conditions are explored, the information and insight needed to optimize the process will be gained.

Acknowledgments

The support for this work provided under a National Science Foundation Graduate Fellowship and by the Department of Energy, Allegheny Power Systems, and Johnson and Sons is gratefully acknowledged. The authors would also like to thank Qian Zhou for helpful advice in matching conditions from her experiments for the hot injection study.

References

Boyle, J., Russell, A., Yao, S.C., Zhou, Q., Ekmann, J., Fu, Y., and Mathur, M. "Reduction of Nitrogen Oxides from Post-Combustion Gases Utilizing Molecular Radical Species," *Fuel*, **72**: 1419-1427 (1993).

Burns and Roe Company. "Preliminary Economic Assessment [of] PETC Radical Injection Process for NO_x/SO_x Control," prepared for Pittsburgh Energy Technology Center, U.S. Department of Energy (July 1992).

101st U.S. Congress. Public Law 101-549 (The 1990 Clean Air Act Amendments).

EPA Office of Air and Radiation. Summary of NOx Control Technologies and their Availability and Extent of Application. EPA-450/3-92-004 (1992a).

EPA Control Technology Center. Evaluation and Costing of NOx Controls for Existing Utility Boilers in the NESCAUM Region. EPA-453/R-92-010 (1992b).

Hahn, W.A., Wendt, J.O.L., and Tyson, T.J., 1981. "Analysis of the Flat Laminar Opposed Jet Diffusion Flame with Finite Rate Detailed Chemical Kinetics," *Combustion Science and Technology*, **27**: 1-17.

Lyon, R.K. "Method for the Reduction of the Concentration of NO in Combustion Effluents Using Ammonia," U.S. Patent No. 3,900,554 assigned to Exxon Research and Engineering Company (August 1975).

Lyon, R.K. "Themal DeNOx," *Environmental Science & Technology*, **21**:231-236 (1987).

Miller, E. and McMillion L.G., 1992. "The Suppression of Opposed-Jet Methane-Air Flames by Methyl Bromide," *Combustion and Flame*, **89**: 37-44.

Offen, G.R., Eskinazi, D., McElroy, M.W., and Maulbetsch, J.S. "Stationary Combustion NOx Control," *Journal of the Air Pollution and Control Association*, **37**:864-870 (1987).

Possiel, Norman C., ed. Regional Ozone Modeling for Northeast Transport (ROMNET). U.S. Environmental Protection Agency Office of Air Quality Planning and Standards (1991).

Potter, A.E. and Butler, J.N., 1959. "A Novel Combustion Measurement Based on the Extinguishment of Diffusion Flames," *ARS Journal*, **29**: 54-56.

Salimian, S. and Hanson, R.K. "A Kinetic Study of NO Removal from Combustion Gases by Injection of NH_i-Containing Compounds," *Combustion Science and Technology*, **23**:225-230 (1980).

Whitten, G.Z. and Hogo, H., 1980. "Modeling of Simulated Photochemical Smog with Kinetic Mechanisms Volume 2. CHEMK: A Computer Modeling Scheme for Chemical Kinetics," U.S. EPA Report No. EPA-600/3-80-026b.

Zhou, Q., Yao, S.C., Russell, A., and Boyle, J. "Flue Gas NO_x Reduction Using Ammonia Radical Injection," *Journal of the Air and Waste Management Association*, **42**: 1193-1197 (1992).

Zhou, Q. "The Effect of Plasma Injection on NO_x Emissions for Pulverized Coal Combustors," Ph.D. Thesis, Carnegie Mellon University, 1991.

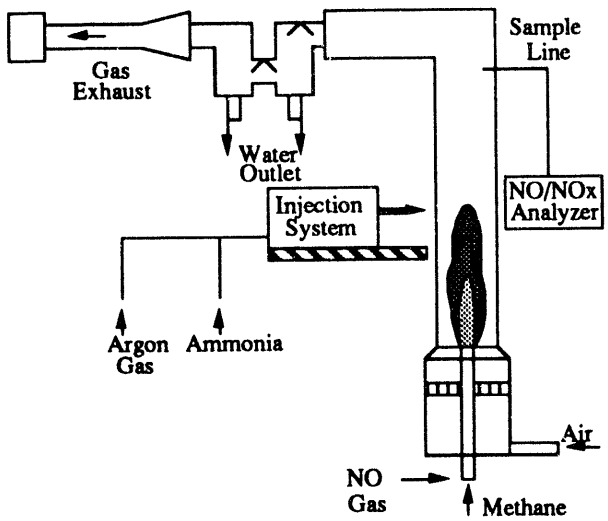

Figure 1. Overall apparatus used in CMU plasma and hot NH3 injection experiments.

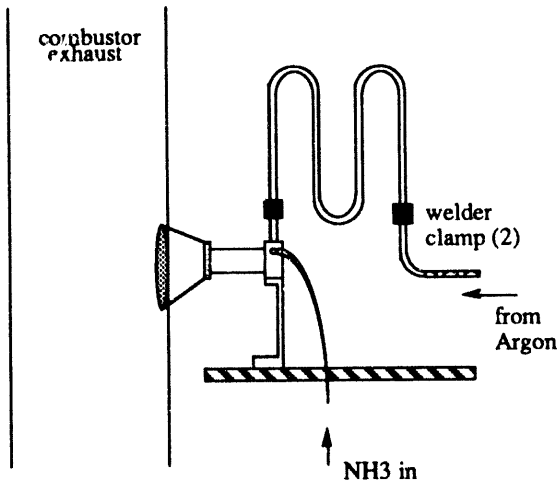

Figure 2. Hot injection apparatus replacing plasma system.

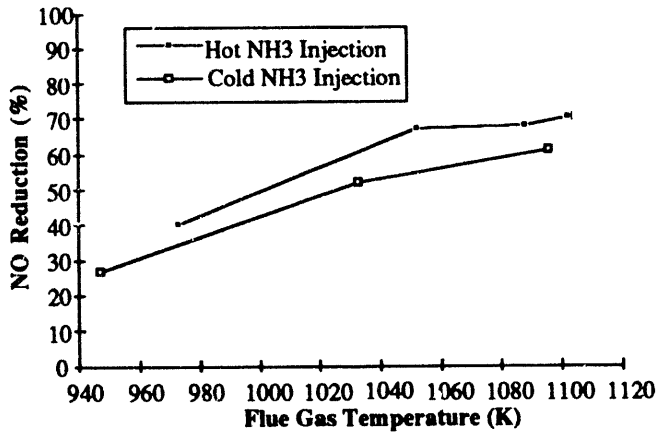

Figure 3. Comparison of cold and hot injection NO reduction at 25% excess air conditions.

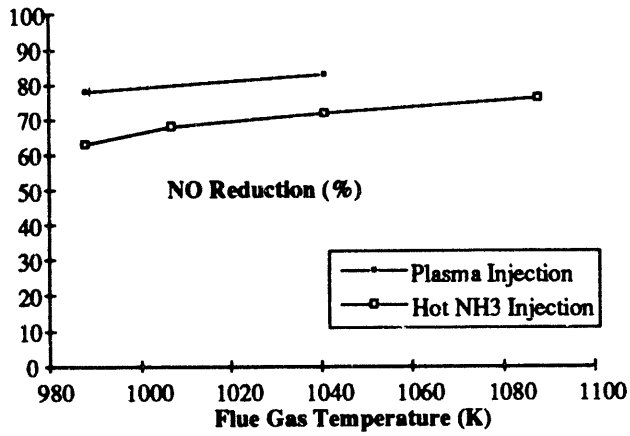

Figure 4. Comparison of hot and plasma injection NO reduction at 0% excess air conditions.

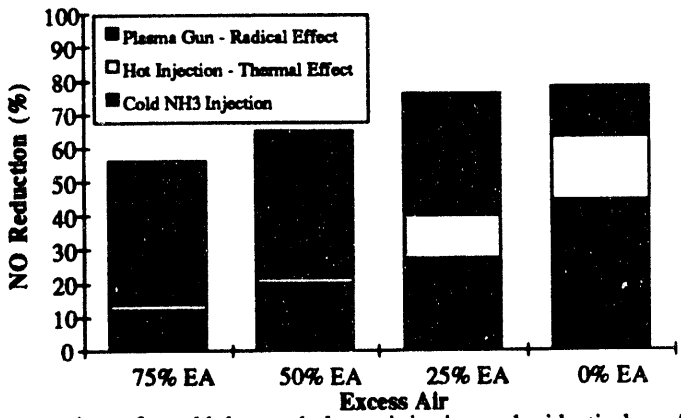

Figure 5. Point comparisons for cold, hot, and plasma injection under identical gas flow conditions.

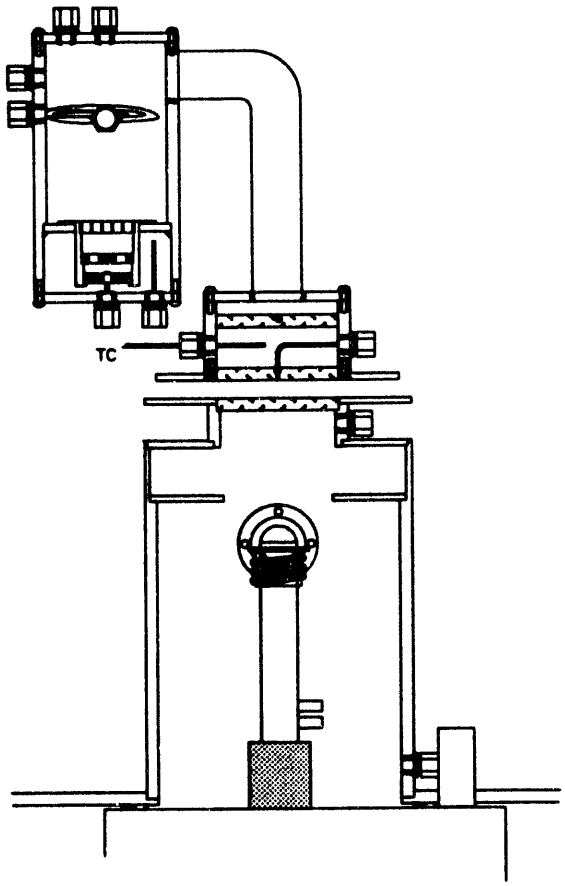

Figure 6: Cross-section view of opposed jet experiment system.

The following manuscript was unavailable at the time of publication.

REGENERATION OF SPENT SCRUBBER LIQUIDS FOR NO_x CONTROL PROCESSES

A. Randolph
University of Arizona
College of Engineering & Mines
Department of Chemical Engineering
Tuscon, AZ 85721

Please contact author(s) for a copy of this paper.

PHOTOSYNTHETIC CONVERSION OF CO_2 TO BIOMASS

Lewis M. Brown, Project Manager
Kathryn G. Zeiler, Staff Scientist
Susan G. Talbot, Technician
and Dana A. Heacox, Technician

National Renewable Energy Laboratory,
1617 Cole Boulevard., Golden, CO 80401

BACKGROUND

Combustion flue gases are the primary contributors to excess carbon dioxide in the atmosphere, a factor which has been linked to possible global climate change. Microalgae potentially could use flue gas as a carbon dioxide feedstock for the solar biological production of biomass (photosynthesis). In microalgae and higher plants, photosynthetic production requires land, water, sunlight and other nutrients. Of the photosynthetic organisms, microalgae are the most productive carbon dioxide users and can fix greater amounts of carbon dioxide per land area than higher plants. Also, maximum productivities of higher plants and trees are restricted to areas with prime soil, water, and climate. Plant leaves exist in an aerial environment and are subject to large evaporative moisture losses, which directly inhibit the process of photosynthesis. Microalgae in mass culture are not subject to such photosynthetic inhibition because the water content of the culture can be controlled by proper engineering, and saline water can be used if necessary. This difference is the basis for the several-fold higher carbon dioxide absorption capacity of microalgae compared to plants.

INTRODUCTION

There is an increasing amount of work being done on the issue of the growth of microalgae in flue gas. Several studies have addressed the growth of microalgae at high levels of CO_2.[1,2,3,4,5,9] An early set of chemostat experiments with the prasinophycean alga *Tetraselmis suecica* employed flue gas collected from a oil-fired generating station collected in large teflon sampling bags then brought to the laboratory for injection into chemostats.[6,7] The algae grew, but the authors suspected that the method of collection of the flue gas resulted in the inclusion of large amounts of air in the flue gas sample.

The effects of a simulated flue gas containing carbon dioxide, sulfur dioxide, nitric oxide and on the growth of some microalgae in culture were investigated.[8] Sulfur dioxide was inhibitory to growth at 400 ppm, but there was some tolerance to and growth in the presence of NO_x supplied as NO at 300 ppm by a *Nannochloris sp.* Sulfur dioxide and nitric oxide were not used in combination in this study. Cultures of *Chlorella vulgaris* and *Tetralselmis suecica* were apparently killed by exposure to a simulated flue gas mixture containing 200 ppm SO_2, while the growth of *Cyanidium caldarium* was severely inhibited.[9]

Field studies indicated that flue gas could be used to grow microalgae in raceway type cultivation.[10,11] A *Phaeodactylum* sp. and *Nannochloropsis* sp. were used in this work. The flue gas (presumably oil-fired) contained 10-12% CO_2 and 70-90 ppm of both SO_x and NO_x. The culture system consisted of raceway type ponds (approx 2 m^2 and 20 cm deep) with paddlewheel mixing. Additional work indicated that microalgae could grow in flue gas composed of 10-15% CO_2 , 70-150 ppm SO_x , and 70-150 ppm NO_x.[12]

Overall, these early laboratory and field results evaluating the ability of microalgae to grow in modest levels of SO_x and NO_x in flue gases or simulated flue gases appear promising. However th888e levels of these potentially inhibitory components have not been studied at concentrations appropriate to, and including, other components that would be derived from, coal-fired generation. The bulk of fossil-steam generated electricity is derived from coal, thus making it important to address microalgal growth upon exposure to coal-derived flue gas. Moreover, the complexities of the chemistry, biology and engineering of these systems has just begun to be addressed.

EXPERIMENTAL WORK

The present work was directed to evaluating the effects of simulated flue gas mixtures on the growth and survival of photosynthetic microbes in culture. A large effort has been directed toward the set-up of laboratory-scale procedures for efficient control of dosing of flue gas into cultures. Efficient control will require the use of an automated system. Computer control will allow the maximum flexibility in the design of experiments and simulated flue gas introduction. The flue gas delivery system requires mixing of the reactive flue gas components containing NO and SO_x in mixtures. Also the resulting mixture must be accurately metered into culture vessels as well as control gases. Our system uses flow controllers from MKS instruments, Model #1259C (Fig. 1). Control of these units is provided by a controller unit µMac #1050 with associated input/output panels (Analog Devices/Azonix). An 80486-class computer running Labtech Control for Microsoft Windows provided software control for these microprocessors (Fig. 2). This system will allow us to provide fine-tuned control of gas mixing and delivery.

Work at NREL using this system has centered on evaluating growth under a variety of conditions and flue gas regimes. Current efforts focus on the optimization of CO_2 uptake and incorporation into biomass.

REFERENCES

1. T.K. Takeuchi, K. Utsunomiya, K. Kobayashi, et al., "Carbon Dioxide Fixation by a unicellular green algae *Oocystis,*" J. Biotechnol, 25:261-267, (1992).

2. H. Takano, H. Takeyama, N. Nakamura, et al., "CO_2 Removal by High Density Culture of a Marine cyanobacterium *Synechococcus* Using an Improved Photobioreactor Employing Light-Diffusing Optical Fibers," Unpublished manuscript, 1992.

3. N. Nishikawa, K. Hon-Nami, A. Hirano, et al., "Reduction of Carbon Dioxide Emission from Flue Gas with Microalgae Cultivation," Energy Convers. Mgmt. 33:553-560 (1992).

4. Y. Watanabe, N. Ohmura, H. Saiki, "Isolation and Determination of Cultural Characteristics

of Microalgae Which Functions under CO_2 Enriched Atmosphere," Energy Convers. Mgmt. 33, pp 545-552 (1992).

5. C. Akin, A. Maka, S. Pradhan, et al., "Technical Report: Removal of CO_2 from flue gas by algae," Contract FC22-92PC9251. DOE/PC/92521--T6. GPO Order no. DE93013625 Office of Scientific and Technical Information, Oak Ridge, TN, p 19 (1993).

6. E. Laws, "Mass Culture of Algae Using carbon Dioxide from Stack Gases," EPRI GS-7029 Project 2612-11, Final Report. October, 1990. Electric Power Research Institute, Palo Alto, CA, 1990, p 104.

7. E.A. Laws, J.L. Berning, "A study of the energetics and economics of microalgal mass culture with the marine chlorophyte *Tetraselmis suecia:* Implications for the use of power plant stack gases. Biotechnol. Bioeng. 37: 936-947 (1991).

8. M. Negoro, N. Shioji, K. Miyamoto, et al., "Growth of microalgae in high CO_2 gas and effects of SO_x and NO_x," Appl. Biochem. Biotech, 28/29, pp 877-886 (1991).

9. J.T. Hauck, G.J. Olson and M.B. Perry, "Effects of Simulated Flue Gas on Growth of Microalgae", Ninth Annual Coal Preparation, Utilization and Environmental Control Contractors Conference, U. S. Dept. of Energy, Pittsburgh, PA, 1993, p 503.

10. Y. Ikuta, Y. Hukuda, M. Negoro, et al., "Carbon dioxide fixation by microalgal photosynthesis using actual flue gas discharged from a boiler", Proceeding of the Fourteenth Symposium on Biotechnology for Fuels and Chemicals, Gatlinburg, TN, 1992.

11. M. Negoro, A. Hamasaki, Y. Ikuta, et al., "Carbon Dioxide Fixation by Microalgal Photosynthesis Using Actual Flue Gas Discharged from a Boiler," Appl. Biochem. Biotech, 39/40, pp 643-653 (1993).

12. A. Hamasaki, N. Shioji, Y. Ikuta, et al., "Carbon Dioxide Fixation by Microalgal Photosynthesis Using Actual Flue Gas Discharged from a Boiler", Unpublished Manuscript, 1993, p 20.

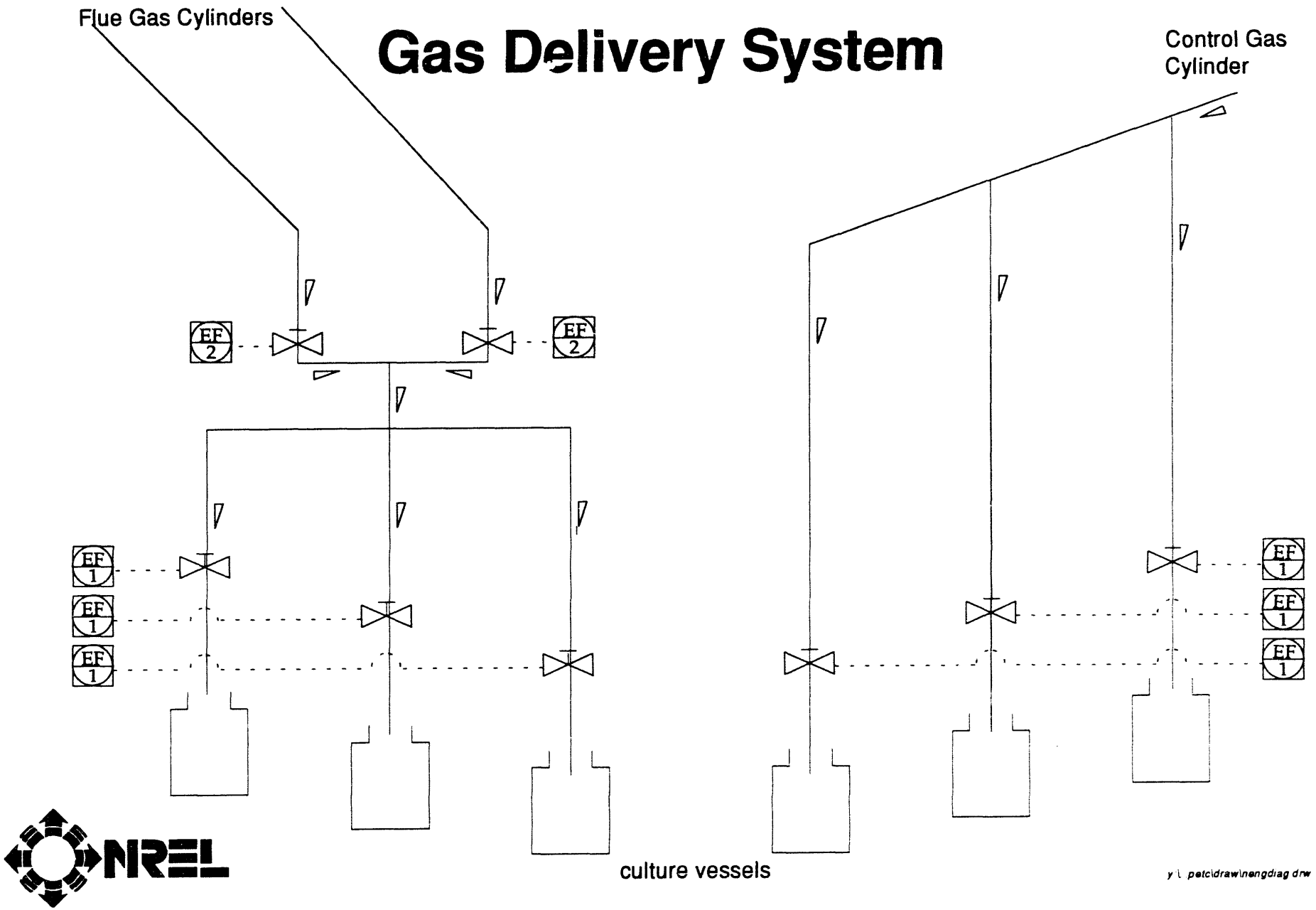

Fig. 1. Diagram of gas delivery system showing valving for flue gas cylinders (left side), and valving for control gas lacking reactive components (right side).

Electronic Schematic

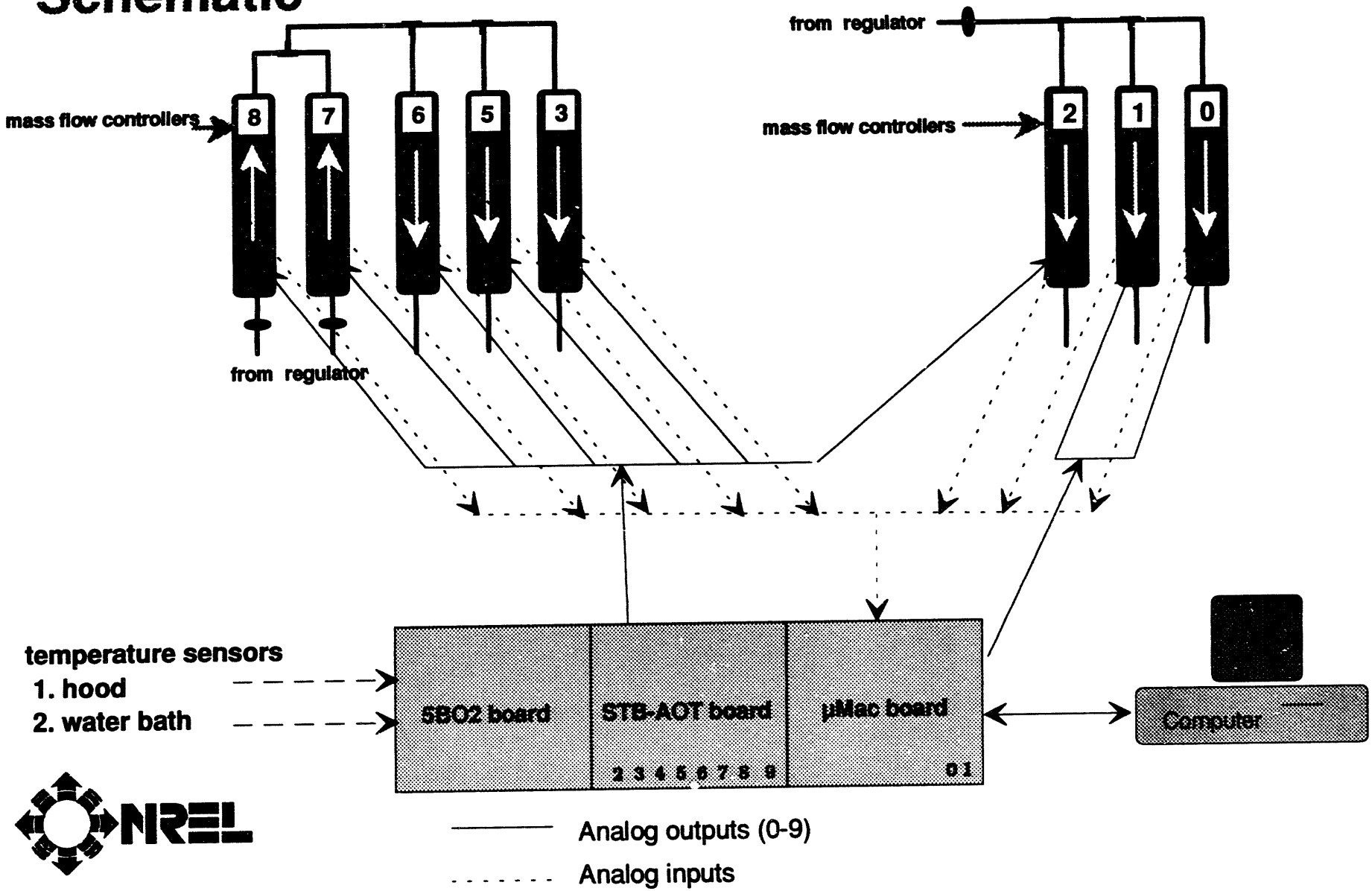

Fig. 2. Schematic of electronic connections used to control gas flows in this system. Valves 0, 1 and 2 are for control gases. Valves 3,5,6,7,8 are for flue gas.

y:\ngroup\aquaproj\petc\draw\2nelectm. drw

The following manuscript was unavailable at the time of publication.

SAMPLING A IGCC PLANT FOR AIR TOXICS

G. Eklund
Radian Corporation
P.O. Box 201088
Austin, TX 78720-1088

Please contact author(s) for a copy of this paper.

The following manuscript was unavailable at the time of publication.

WESTON VIDEO

B. Jackson
Roy F. Weston, Incorporated
One Weston Way
West Chester, PA 19380-1499

Please contact author(s) for a copy of this paper.

AN ONLINE OPTICAL MONITORING OF AIR TOXICS

VAL K. BYKOVSKI
DIRECTOR OF RESEARCH
VIRTEK CO. AND UNIVERSITY OF MASSACHUSETTS AT LOWELL

ABSTRACT

New methods are needed to analyze and monitor *multicomponent*, for example, air toxic mixtures. The existing methods are basically a single-pass measurement and do not provide enough information. We propose an optical exploration approach, *a multi-step feedback controlled technique* that includes multiple measurements with *systematic modification* of mixture to get additional data. We discuss various optical techniques to modify and probe air toxic mixtures. The data obtained from the multiple measurements allow the individual concentrations to be evaluated. Experimental data on the feasibility Phase I project are presented.

1. INTRODUCTION AND BACKGROUND

The large-scale industrial processes such as combustion, incineration, etc., generate large amounts of air toxics. The impact of air toxics, in particular, mercury and other metals on health risks may be significant for the entire US population. The paper addresses the need to develop efficient means to analyze and monitor complex, multicomponent mixtures, for examples, air toxics, ambient environments, etc. Air toxics [N91,C91] is a complex, reactive mixture of various chemical components in various states such as micro and nanoparticles, aerosols, molecular clusters and complexes. Its analysis and monitoring is a challenging problem that requires an innovative approach. While a number of methods and instruments are available to analyze and monitor air toxics (ATs)[C91,C91a], the problem of their reliable continuous monitoring is far from a solution[W90,N91,C91]. The existing methods (see, for example, [W90]) need improvement in terms of reliability, selectivity, and performance. An online, real-time monitoring is needed to provide early warning and, potentially, online removing of health risky components.

In the previous paper [B93], we have proposed a method for online monitoring air toxics mixtures that includes the multiple measurements with a systematic optical modification of the mixture. The present paper makes the next step in the same direction and considers an innovative *active, optical system* for analysis and continuous monitoring of air toxic mixtures. Its basic idea is that a single-pass ("shoot-and-forget") measurement is replaced by a *multi-step feedback controlled exploration* of an unknown mixture X. The proposed measurement architecture includes: (1) a set of probing sources; (2) a set of sensors or detectors; (3) a set of advanced *effectors* - facilities for *in-situ modification* of the object to be analyzed, and (4) system controller - a facility to control system operations, process data, and make decisions on a current step. An integration of all these features into a flexible architecture for optical exploration would open a new dimension in online/in-situ analysis and monitoring for environmental applications.

The proposed method has two innovative features: (1) a single-pass measurement for the mixture is replaced by a *sequence* of measurements with *in-situ* prepared mixtures that allow the composition of the mixture to be reconstructed computationally based on the multiple measurements; and (2) a *fixed* effector/detector (E/D) pair is replaced by a pair to be chosen depending on currently available (missing) information; a probing beam characteristics such as a spectrum (say, single line, white source, etc) can also be dynamically set up. An *effector* (modifier) has *capabilities* to excite X into different electronic (vibrational and/or rotational) states X_i. A proper sensor/detector measures a desirable property $P(X_i)$ in *a probing mode*, and the system, then, *evaluates* the current results and makes decision on the next step. We also consider optical *addressing and processing options*, that is, how to pick up optically a specific component in a mixture and perform a specific optically-induced (chemical) transformation.

2. APPROACH

The reliable monitoring of multicomponent gas flows requires measuring concentrations of individual components such as air toxics (ATs), VOCs, etc. A spectrum of a mixture is to be interpreted in terms of spectra of individual components, and, then in terms of their concentrations. This problem, though, doesn't have a unique solution. That is, a spectrum of a mixture is simply not enough to determine its composition. A standard *approximate* technique is to assign different peaks in the spectrum to different components and then to compute the components' quantities based on peak intensities. This does make sense if the spectrum is a combination of *non-overlapping* peaks of different components. However, in real situations an overlap often makes the assignment difficult. For example, in the case of gasification streams, the IR peaks of HCl and CH_4 are significantly overlapped. Intensive and wide-range water vapor absorption is another complication.

The proposed method resolves this problem. It replaces a single measurement by a *controlled* sequence of measurements, that is, by a flexible program in which every measuring step may depend on results of previous measurements. The measurement system is designed so that a ATs mixture can be prepared *in-situ* in *different states*, then the *in-situ* measurement is made to get *additional* data needed, say, to compute individual concentrations. External lasers can be used to heat up the mixture, excite it optically in different states, etc. Indeed, the optical parameters of a mixture are changed but its *composition* is essentially *the same*.

The different *in-situ* preparation techniques can be used. For example, (1) a *new known* component can be injected in the *known amount*; or (2) one of the present components can be modified optically, or (3) a component can be removed optically and/or chemically. The exploration program first controls preparation of a "new mixture" and then does a measurement, repeating a cycle *preparation- measurement-evaluation* until *all* needed information is obtained to compute, say, the components' concentrations of the mixture.

Another environmentally important option is an *action* in response to the detection of a component. For example, an *in-situ* response may include the optical control of the component's chemical reactivity, adsorptivity, particles cohesion, clustering, etc. A challenging opportunity

would be to use optically-induced processes such as (photo) polymerization, depolymerization, decomposition, clusterization, adsorption, absorption, precipitation, etc. to *remove* pollutants from the mixture. The photoinduced removal process can be triggered when a measurement has detected unacceptable amount of a pollutant.

The flexibility and reliability are important features of the proposed method. For example, the measurement program can be designed to monitor different air toxics using different schedules; say, *Hg* and *Pb*, two air toxics that are of most health risk concern, can be monitored, say, once a 10 *s* whereas other air toxics once every 10 *min*. The program may speed up monitoring if concentration of a pollutant goes up and may expand the number of pollutants to be monitored if a specific pattern of pollution emerges. The program can as well be in a "sleeping", *change-only* monitoring mode switching in a multi-step exploration mode when a sharp change is detected. The reliability is another useful feature. If a measurement turns out to be unable to resolve uncertainty due to the overlap between two or more components, the measurement program can initiate additional measurements with the properly prepared mixtures to refine the result to match a prespecified reliability (or any other) criterion. Conventional measurements do not offer such flexibility and reliability. For example, in the IR spectral measurements, the overlap between a HCl peak and the peaks of other components, say, methane CH_4 as well as water vapor contribution may make monitoring unreliable. In this case, the proposed method utilizes an external laser to prepare a modified mixture. The laser hits HCl in its absorption band. That causes a selective excitation of HCl, and enhances its refractive index RI. Then, the measurement is done with the new mixture in which HCl component is optically enhanced and separated from CH_4 component so that HCl provides a main contribution into currently measured RI.

The high performance is last (but not least) useful feature of the proposed ATs optical monitoring method. Typically, a single optical measurement can be done in few milliseconds time and even less. That allows the multiple controlled measurements to be done in very short time, and makes the ATs monitoring a high performance data acquisition process. In other words, the optical exploration is a high speed technology that can be characterized by the number of elementary steps done in a second. It is reasonable to expect that in many practical cases the performance may be in a range of 1-10K op/s and more.

Air Toxics Monitor. For ATs monitoring, an efficient effector/detector pair may include a tunable laser diode (LD) (or a set of LDs for various wavelength ranges) and a Zeeman interferometric refractive index (RI) detector. In a laboratory prorotype built within the SBIR Phase I feasibility study, we actually used a monochromator to excite optically an ATs mixture using different wavelengths. The probing beam as well as a reference frequency is specified by a two-frequency Zeeman laser. We used a He-Ne laser with the magnetic frequency splitting 250 kHz (Optra, Peabody, MA). This combination provides sensitivity, high speed, robustness, and universality. The Zeeman RI detector is a *universal* one as it is applicable to any transparent enough mixture, doesn't depend on specific chemicals, and specific properties such as fluorescence, conductance, etc. The Zeeman laser based RI detector has been extensively studied by Roger Johnston's group at the Los Alamos National Laboratory [J90]. The proposed measurement method is an interferometric one, and among many interferometric methods it is a

phase-sensitive rather than *intensity-sensitive*. This is an essential advantage, as a phase-sensitive detector operates in a synchronous (lock-in) detection mode that filters out all noise beyond a reference frequency. That makes the method unique in terms of *reliability and sensitivity*, features that are important for any practical analysis and monitoring system. In other words, the proposed monitoring technique is the best possible one for this class of measurement systems.

An intensity based detector such as Fourier Transform IR (FTIR) would also be a useful module in the proposed multimodule monitoring system giving a *complementary* information to test a hypothesis about the ATs composition. It can be combined with a white light probing beam, an appropriate effector, say, a pulse laser diode, and an array photodetector.

A single measurement with an ATs mixture gives an average RI, n, of the mixture in which all components contribute:

$$n = \sum_{i=1}^{N} c_i n_i(s)$$

where c_i is the concentration of the i-th component, and N is the total number of components in a mixture. The single measurement is not enough to compute N individual concentrations c_i. However, the components' RIs, $n_i(s)$, depend significantly on the specific electronic state s of a component. By *selective optical excitation*, the mixture can be prepared *in-situ* so that a contribution, in n, of a specific component 0, say, *Hg*, will be *enhanced* significantly, that is:

$$n = c_0 n_0 + \sum_{i \neq 0}^{N} c_i n_i(s)$$

In this sum, only the i=0 component contributes significantly as all $n_i << n_0$. This is due to the fact that according to the Sellmeier formula

$$n^2(\lambda) = \alpha + \beta\lambda^2/(\lambda^2 - \lambda^2_0)$$

where λ is the wavelength of the exciting radiation, λ_0 is the resonant wavelength for a specific component *0*, and α and β material parameters for the component *0*. In other words, when the excitation wavelength λ approaches to the resonant wavelength λ_0, the RI may become very large.

If a detailed information is required about all components, then a sequence of measurements is to be made. The series of N measurements generates a set of N equations that allow the N concentrations to be calculated by solving the following set of equations:

$$\sum_{i=1}^{N} c_i n_{im} = n_m, \qquad m = 1..M$$

where N is the total number of components in a mixture, c_i is the concentration of the i-th component, n_m is the RI of the mixture in the measurement m, and n_{im} is the RI of the component i in the measurement m. If $N = M$, that is, the number of measurements M equals the number of

components N, the set of equations is unique and allows the all components' concentrations c_i to be calculated. If $M > N$, the set of equations is overdefined, and that allows the components concentrations c_i to be tested additionally for robustness. So, the multiple measurements give an additional information about the mixture and allow the composition to be reconstructed computationally by solving a set of algebraic equations online with the measurements. The right-side terms of the set are the result of *multiple* measurements. This information simply cannot be obtained from a single measurement.

3. DISCUSSION AND RESULTS

A block diagram of the proposed exploration architecture is shown in **Fig. 1**.

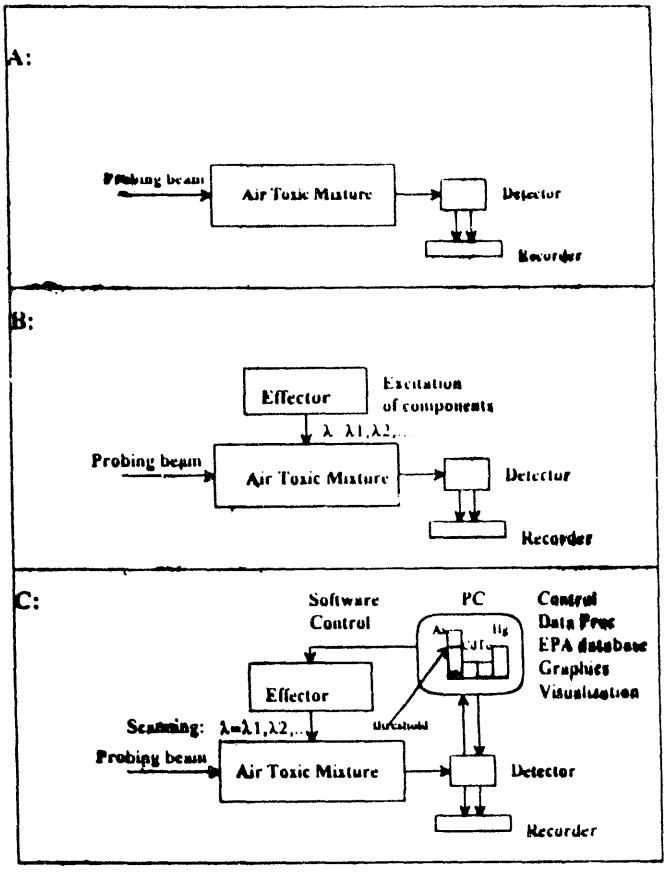

Fig.1. Evolution of measurement architectures: single-pass (A), multi-pass (B), and controlled multiple optical measurements

The RI detector measures changes in refractive index (RI), n, of a sample such as flowing gas or liquid. The dimensionless number $n = v/c$ equals the ratio of the speed of light in vacuum c to the speed of light in the medium. For example, $n = 1.000293$ for pure air, $n = 1.000034$ for helium. The RI detector can typically detect *ppm*-changes in the concentration of gaseous contaminants in air, and *ppb*-changes for contaminants in liquids.

The *relative* measurements are easily accomplished with the RI detector, say, a current gas sample relatively a "reference" one that contain allowable components in proper proportions.

For example, the reference sample may contain an allowable mixture of pollutants, and the instrument will detect any changes in a gas flow *vs.* to the reference mixture. The detector can also be operated in a *differential* mode. The flowing gas first enters a sample chamber, then immediately enters a reference chamber. This is useful for distinguishing the transient changes in RI. In this mode, instead of recording a peak, the instrument records the derivative of the peak. The RI detector is (1) ultrasensitive: measures changes in RI as small as 10^{-9}; (2) linear over entire operating range; (3) self-calibrating; (4) simple and robust; (5) has an outstanding stability; (6) no electronic, optical or mechanical adjustments necessary after initial assembly; (7) can track changes in RI millions of times larger than its resolution. The RI detector can be used as a monitor of the *constancy of composition* of flowing gases, liquids, and industrial discharges. A block-diagram of the RI detector is presented at **Fig.2.**

In addition to a low power He-Ne laser probe beam, an external excitation laser is used to modify a mixture and change its RI. The connection between a change in the phase of the beat frequency, $\Delta\phi$, and a change in ΔT, in the relative temperatures of the heated and unheated portions of the sample is

$$\Delta\phi = 360^{\circ} L/\lambda \, \Delta n,$$

where Δn is the change in the RI because of optical excitation, L is the average path length in the probe volume (L=*50 mm*), and λ = 632.8 nm. For example, to detect *Hg*, all that is needed is to hit the gas sample with an excitation beam that is absorbed by *Hg*. The change in RI of the whole mixture caused by the excitation and heating of *Hg* can be used to infer the change in *Hg* concentration.

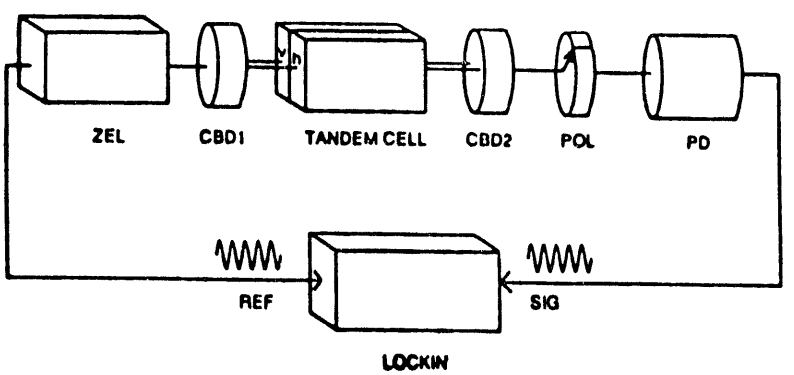

Fig.2. The RI detector. ZEL is the Zeeman laser, CBD1 and CBD2 are the beam displacers, POL is the polarizing analyzer, and PD is the photodetector

Virtually any contaminant can be detected independent of special properties like fluorescence, electrical conductivity, chirality, or absorption bands. An example of detecting Freon-12 gas (CCl_2F_2) in air (**Fig.3**) shows that the minimum detectable concentration of Freon-12 using this technique (for L = 50 *mm*) is 0.2 *ppm*.

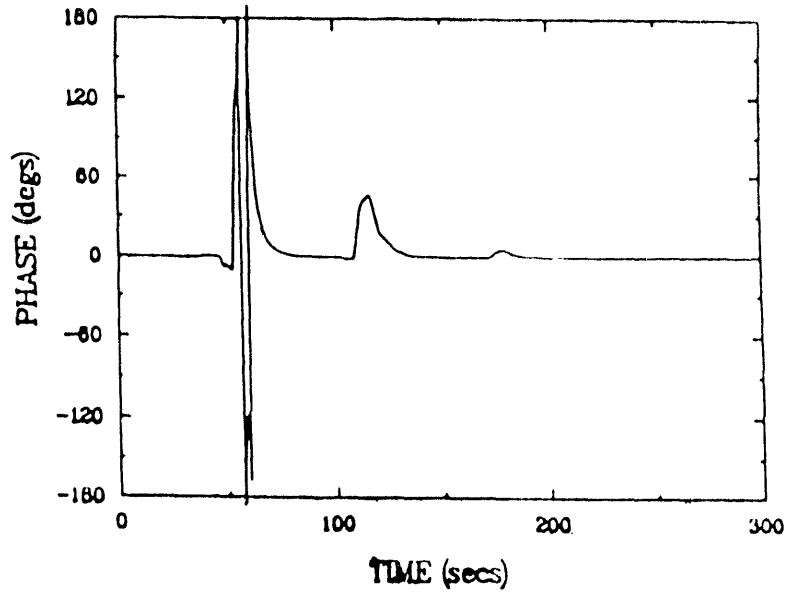

Fig.3 The detection of Freon-12 gas in air at peak concentrations of 800, 150, and 15 *ppm* at 60, 120, and 180 *s*, respectively. The minimum detectable concentration is 0.2 *ppm*

Fig.4 shows results of optical modification of Hg/methanol/air ATs mixture. Curve 1 shows the RI dynamics without external radiation. The changes are due to the periodical injection of mercury vapor into the sample beam by a gas syringe filled with the mercury vapor. Curve 2 shows an optical enhancement of the same RI changes due to the external resonance radiation (mercury green line 436 *nm*). A cylindrical lens was used to expand the excitation beam to maximize the interaction volume between the sample and excitation beams.

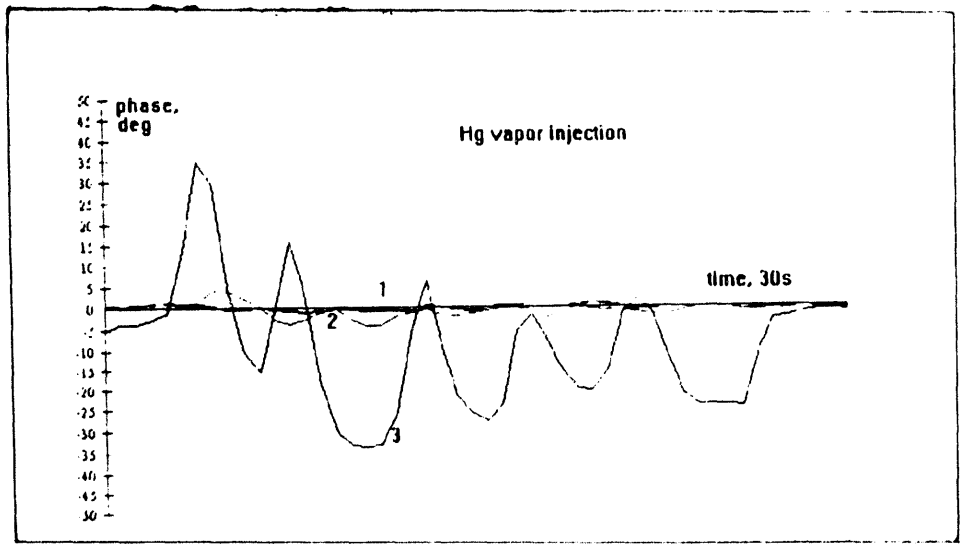

Fig.4. Optical enhancement of mercury' RI in Hg/CH_3OH/air mixture by resonance radiation

4. CONCLUSIONS

An optical technology is a "dry" (as opposed to wet chemical technologies), high speed, and easily controlled one. The optical methods are promising as well as a future *control technology* that allows the ATs to be optically transformed and/or removed *in-situ* using optical control of chemical reactivity of ATs. The proposed ATs monitor will allow the power plants, utilities, incinerators, and other ATs generating sources to reliably monitor ATs [C91,C91a,N91]. In a closed-loop process control system, the method can be used to *control* combustion, incineration, and other ATs generating processes to provide a *prespecified* level of ATs emissions in the gas stacks. In combination with complimentary weather data records (such as winds and precipitation dynamics), it would allow the sources of pollution to be detected.

5. ACKNOWLEDGEMENT

Authors thank Dr. Roger Johnston of Los Alamos National Laboratory for helpful discussions of the proposed method and suggestions on the measurement strategy. They also thank Prof. Mike Fiddy and Prof. Mike Ellenbecker of University of Massachusetts at Lowell for discussions. Mr. Ralph Mongeon, Manager at Riley Stoker Research, Worcester, MA, has contributed significantly in shaping the air toxics monitoring environment. His input is highly appreciated. Advice and encouraging by Dr. Leo Smolensky of LSR Technologies, Acton, MA, were very helpful. Author also thanks Optra, Inc. for lending a He-Ne 2-frequency laser. The research is supported by the US Department of Energy (PETC) under contract No.DE-FG02-93ER81534, and the author appreciate a valuable input from DOE Project Manager Ms. Felixa Eskey.

6. REFERENCES

[B93]. V.K. Bykovski, S.S Choi, "An Online Exploration of Air Toxic Mixtures", Presented at the *SPIE International Symposium on Optical Sensing for Environmental Monitoring* (October 11-15, 1993, Atlanta, GA), SPIE Proc. v.xxx, 1994

[C91]. E.J. Calabrese, E.M. Kenyon, "Air Toxics and Risk Assessment", Lewis Publ., 1991

[C91a]. Constantinou E., Seigner C., "Multimedia Health Risk Assessment for Power Plant Air Toxic Emissions", *Paper presented at the conference on Managing Hazardous Air Pollutants: State of the Art, Washington, DC, Nov. 1991*

[J90]. R. G. Johnston, W. Kevin Grace, "Refractive Index Detector Using Zeeman Interferometry", *Appl. Opt.* **31**, n31, 1990, pp.4720-24

[N91]. "New Focus on Air Toxics", EPRI Journal, March 1991

[W90]. J. K. Wachter, "Air Toxics: Instrumentation Needs". In *Proc. of the 10th Annual Gasification and Gas Stream Cleanup Systems Contractors Review Meeting, v.1, Eds: V.P. Kothari, J.L. Beeson, August 1990, Sponsored by US DOE, Office of Fossil Energy, Morgantown Energy Technology Center, Morgantown, W. Virginia*

THE BEHAVIOR OF CO_2 UNDER SIMULATED DEEP OCEAN CONDITIONS

Anthony V. Cugini and Robert P. Warzinski
U. S. Department of Energy
Pittsburgh Energy Technology Center
Pittsburgh, PA 15236

Gerald D. Holder
Department of Chemical and Petroleum Engineering
University of Pittsburgh
Pittsburgh, PA 15261

Background: Anthropogenic emissions of CO_2 may adversely affect the environment in the not-too-distant future. If this occurs before nonfossil energy sources are developed, we may be forced to consider sequestering CO_2, especially that emitted by large point sources such as power plants. Currently, no options exist for long-term storage of large quantities of CO_2. Establishing the technical feasibility of such large land and ocean storage options has been identified as a high priority research need (1). Even opponents of fossil fuel use for power generation agree that such research is needed in order to allow making correct international decisions (2).

Ocean disposal of anthropogenic CO_2 emissions has the potential of sequestering CO_2 for time periods long enough to mitigate its anticipated buildup in the atmosphere over the next 200 years (1). The level of reduction depends on the relative amount released into the ocean and the depth of discharge. Effective sequestering of CO_2 in the ocean is expected if release depths are greater than 1000 m, which is also near the limit of current undersea piping technology. Uncertainty associated with the physical behavior of CO_2 under these conditions complicates modeling efforts. A better understanding of the miscibility of liquid CO_2 with seawater and of the kinetics of formation and dissolution of CO_2 hydrates under deep-ocean conditions is needed. Miscibility data are important in estimating the residence time and distribution characteristics of liquid CO_2 in deep-sea environments. Information on hydrate formation is important since these solids should be more dense than seawater and therefore sink to the ocean bottom, resulting in very long CO_2 residence times in the ocean. The objective of the work on this project is to obtain information on the dynamics of formation and dissolution of CO_2 hydrates in sea water that would be useful in determining whether deep-ocean disposal of anthropogenic CO_2 emissions is a viable option for mitigating a rise in atmospheric CO_2 levels owing to fossil fuel combustion.

Accomplishments: The behavior of CO_2 in water under conditions similar to those anticipated for deep-ocean disposal has been observed in a high-pressure, variable-volume view cell. A diagram of the view cell system is shown in Figure 1. Figure 2 contains more detail on the view cell itself. Hydrate formation and dissolution have been observed to occur in this system according to published phase behavior data for this system. Observations of the relative density of CO_2 clathrate hydrates with respect to the CO_2-saturated water from which they were formed have also been made in the view cell. Upon formation of the

hydrates at the gas/liquid interface, the hydrates tended to float in the cell. However, with additional time the hydrates became more dense than the liquid phase and sank. The physical appearance of the hydrates also changed with time. Initially, they were white, snow-like particles; later they became transparent like ice. Theoretically, CO_2 hydrates should be more dense than water or sea water and sink. Understanding the dynamics of hydrate formation under deep-ocean disposal conditions is important in predicting the ultimate fate of these particles.

A mathematical model of the effect of hydrate formation on liquid CO_2 droplets is also being developed. Based upon this model, the path of hydrate-coated CO_2 droplets at various depths can be determined. Under certain conditions the formation of hydrates can result in particles dense enough to sink in the ocean. Most of the work in the literature that attempts to predict the fate of CO_2 droplets injected at various depths in the ocean does not incorporate hydrate formation into the models.

Plans: Near-term plans include continuation of the work to verify operation of the view cell against literature data for CO_2-hydrate phase behavior. Modifications of the view cell will also be pursued to enable observation of hydrate formation on individual CO_2 droplets. Additional effort will also be directed at refining the mathematical model to better predict the fate of CO_2 injected into the ocean.

Long-range plans include the development of a state-of-the-art system for studying the dynamics of the formation and dissolution of CO_2 hydrates under conditions similar to those anticipated for deep-ocean disposal of CO_2. The goal is to obtain the necessary experimental data to develop a realistic model capable of predicting the fate of large quantities of CO_2 in deep-ocean environments.

References:

1. DOE Report DOE/ER-30194, July 1993, prepared under Grant No. DE-FG02-92ER30194.A000 (available NTIS).

2. Hangebrauck, R. P. Energy Convers. Mgmt., **1993**, 34(9-11), 737-744.

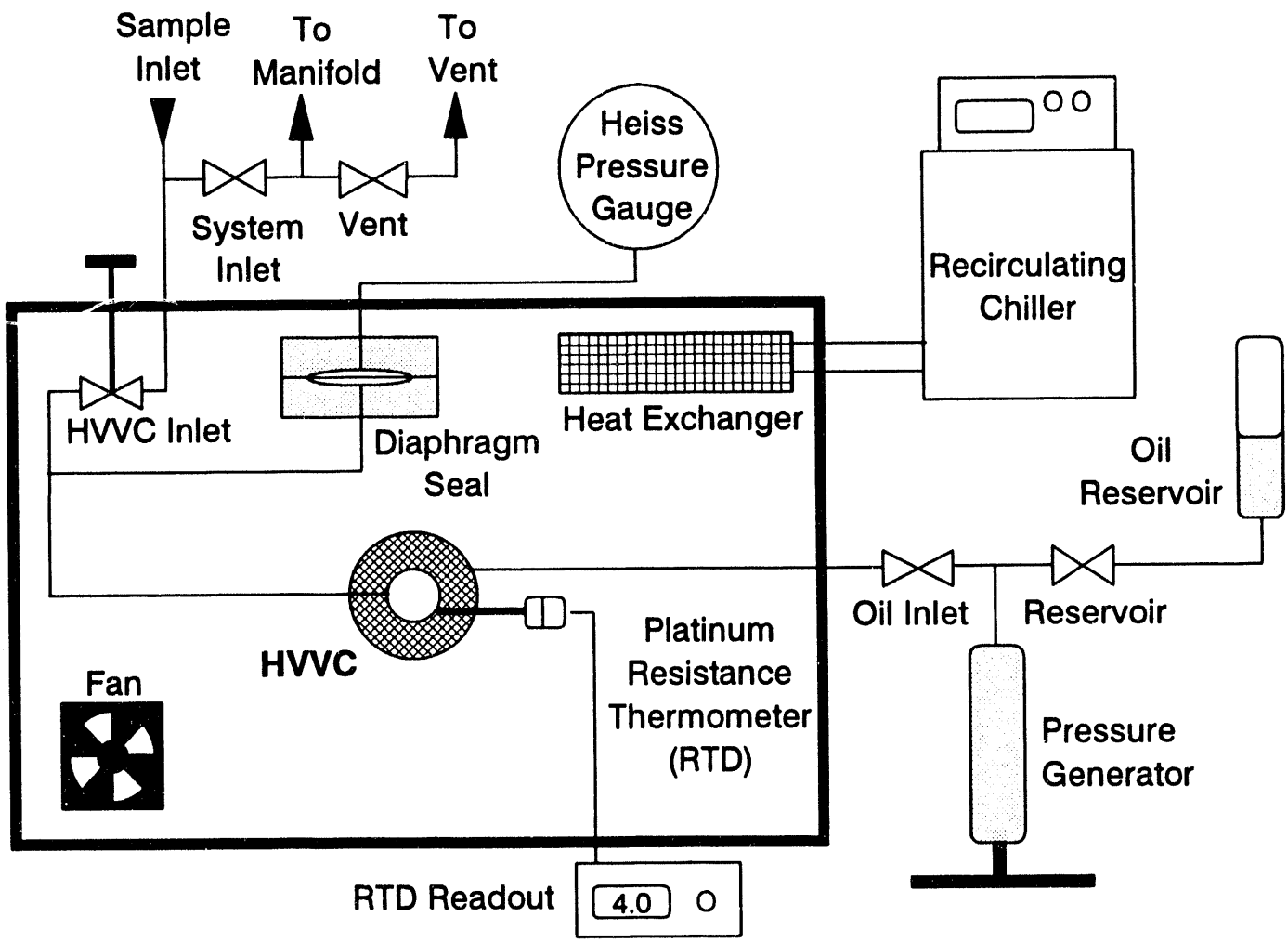

Figure 1. Diagram of the High-Pressure, Variable-Volume View Cell (HVVC) system.

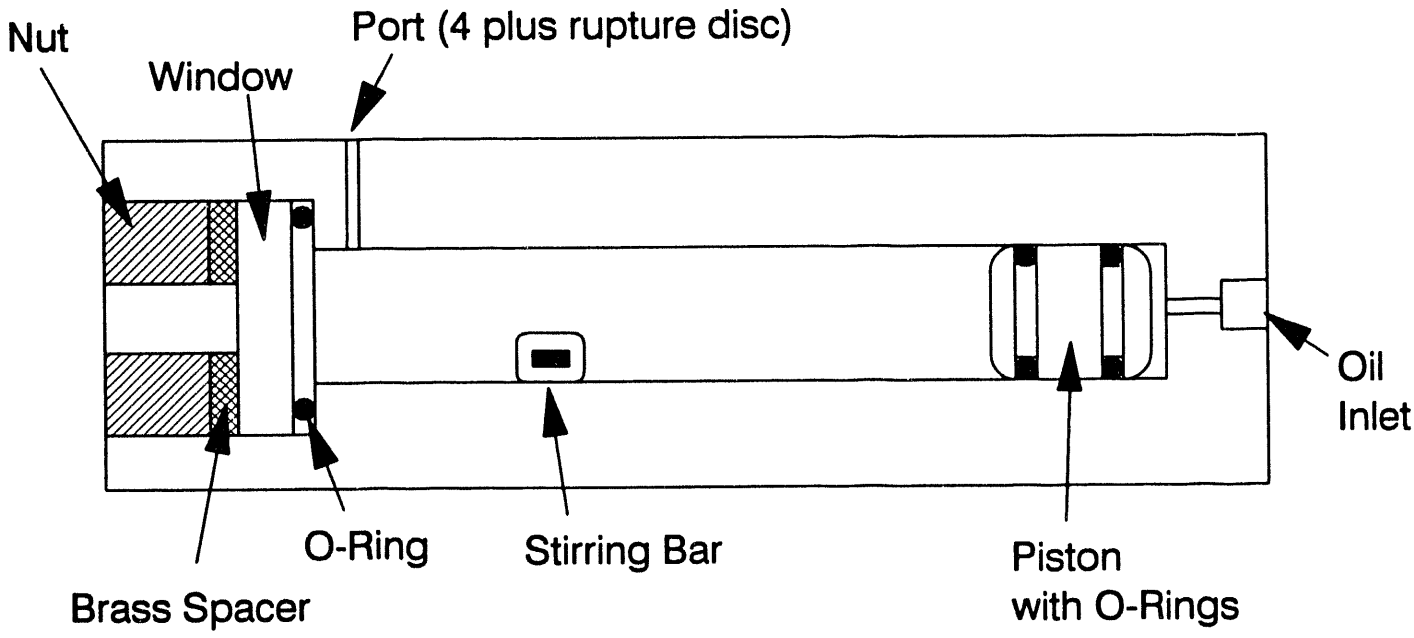

Figure 2. Diagram of the High-Pressure, Variable-Volume Viewcell.

ADVANCED COMBUSTION TECHNOLOGY POSTER SESSION

The following manuscript was unavailable at the time of publication.

DEVELOPMENT OF A LOW-NO_x PULVERIZED COAL BURNER

P. Loftus
Arthur D. Little, Incorporated
Acorn Park
Cambridge, MA 02140-2390

Please contact author(s) for a copy of this paper.

The following manuscript was unavailable at the time of publication.

FEASIBILITY STUDY FOR AN ADVANCED COAL-FIRED HEAT EXCHANGER/GAS TURBINE TOPPING CYCLE FOR A HIGH EFFICIENCY POWER PLANT

P. Solomon
Advanced Fuel Research, Incorporated
P.O. Box 380379
East Hartford, CT 06138-0379

Please contact author(s) for a copy of this paper.

REDUCTION OF NITROGEN OXIDES IN THE NOXSO PROCESS

Q. ZHOU, J. HASLBECK, L. NEAL, S. HARKINS, A. CHANG, and J. BLACK
NOXSO CORPORATION
2414 LYTLE ROAD
BETHEL PARK, PA 15102

Introduction

The NOXSO Process is a dry, post-combustion flue gas treatment technology which can simultaneously remove 90% NO_x/SO_2 using a dry, regenerable sorbent. In the process, NO_x and SO_2 are adsorbed by a fluidized bed of sorbent in an adsorber at a temperature of 120°C. The NO_x is then desorbed by heating the sorbent in a heater and returned to the boiler to be reduced to nitrogen and oxygen. This is called NO_x recycle. SO_2 is regenerated at 620°C using a reducing gas in a regenerator and converted to a sulfur by-product in a Claus plant. After sulfur regeneration, the sorbent is cooled and transported to the adsorber for reuse. The schematic of the NOXSO Process is shown in Figure 1.

Elements of the NOXSO Process have been successfully tested at four different scales since 1979, equivalent to 0.017, 0.06, 0.75 and 5.0 MW of flue gas generated from a coal-fired power plant. The bench-scale tests (0.017 MW) were conducted at the TVA Shawnee Steam Plant.[1,2] Tests of a NOXSO Process Development Unit (PDU, 0.75 MW) were performed at the DOE - Pittsburgh Energy Technology Center (PETC) in a scaled-up process.[3] A Life-Cycle Test Unit (LCTU, 0.06 MW) was built at PETC in 1988 to test the NOXSO Process in an integrated, continuous-operation mode to determine sorbent physical and chemical performance over repeated cycles of adsorption and regeneration.[4] A Proof-of-Concept (POC) pilot scale test was recently completed at Ohio Edison's Toronto Power Plant in Toronto, Ohio. This was the last step prior to a full-scale commercialization plant. A slip stream of flue gas equivalent to a 5 MW coal-fired power plant was used for the POC test. A maximum of 99% SO_2 and 95% NO_x adsorption efficiency was demonstrated during 6500 hours of process operation.[5] A separate pilot scale test of NO_x recycle was also conducted on a 1.7 MW cyclone furnace at Babcock & Wilcox (B&W) Research Center. NO_x recycle was not demonstrated in the POC test since only a fraction of the flue gas from the host boiler was treated at the POC. This paper presents the concept of the process and pilot-scale test data with emphasis on the NO_x reduction in the NOXSO Process.

NO_x Adsorption and Desorption

The NOXSO sorbent is a γ-alumina sphere impregnated with sodium carbonate, Na_2CO_3 on the surface of the sphere. The sorbent is stable, inert, non-toxic and non-combustible. Both sodium and alumina contribute to the NOXSO sorbent's capacity to adsorb NO_x and SO_2 from flue gas. The following mechanism is proposed for the NO_x adsorption according to the experimental findings.

$$Na_2O + SO_2 + NO + O_2 \rightarrow Na_2SO_4 + NO_2 \quad (1)$$

$$Na_2O + 3\ NO_2 \rightarrow 2\ NaNO_3 + NO \quad (2)$$

Figure 2 is a plot of NO_x adsorption efficiency versus the flue gas to sorbent mass ratio obtained during the POC test. The plot shows three data sets: a one-stage adsorber, a two-stage adsorber (two fluid beds in series), and a two-stage adsorber with in-bed water spray to reduce the operating temperature in the fluid bed. The one-stage data show that NO_x adsorption efficiency decreases in proportion to the increase in mass ratio. The two-stage data show the same trend but NO_x adsorption efficiencies are higher by 5 to 10 absolute percentage points. This improvement is due to 1) better gas distribution with the addition of the second grid plate, and 2) counter-current flow of flue gas and sorbent so that in the bottom bed of the adsorber partially spent sorbent is in contact with the highest concentration of pollutants. The figure also shows the effect of adsorber bed temperature on NO_x removal. Data obtained over an adsorber bed temperature range of 120-180°C show a definite trend of increasing adsorption efficiency with decreasing bed temperature. Further improvement is anticipated at bed temperatures lower than 120°C. A NO_x adsorption efficiency of 95% at a flue gas to sorbent ratio of 4.6 was achieved with the two-stage fluid bed including in-bed water spray.

When the spent sorbent is heated by an air stream in the sorbent heater, the adsorbed NO_x is evolved, producing both NO (30%) and NO_2 (70%). The desorption of NO_x occurs according to the following proposed reactions.

$$2\ NaNO_3 \rightarrow Na_2O + NO_2 + \frac{1}{2}O_2 \quad (3)$$

$$2\ NaNO_3 \rightarrow Na_2O + NO_2 + NO + O_2 \quad (4)$$

Laboratory studies showed that NO_x desorption is completed in a fixed bed reactor around 370°C. In the POC tests, the NO_x mass balance between the adsorber and the sorbent heater (620°C) was consistently within 100 ± 15% closure.

NO_x Recycle

The desorbed NO_x concentration is very high because the air stream used to heat the sorbent is a much smaller volume of gas than the original flue gas stream. This NO_x-laden stream is then fed back to the boiler as NO_x recycle. Recycled NO_x is partially converted to nitrogen and oxygen in the furnace because 1) it increases the reverse reaction rate of NO_x formation due to high initial NO_x concentration and thus the net NO_x production rate is inhibited; 2) when the recycled NO_x enters the high temperature fuel rich zones in the flame, free reducing radicals, such as $CH\cdot$, and $CH_2\cdot$, etc., react with the NO_x species, reducing NO_x.

The NO_x recycle concept was first evaluated by conducting a series of simulated NO recycle tests on a 500 lb/hr pulverized coal (PC) combustor and a tunnel furnace at DOE-

PETC.[2] Bottled NO gas was injected into the combustor from the combustion air duct with varying NO_x concentrations. The flow rate of NO_x fed into the combustor and the NO_x concentration at the exit of the combustion system were measured. The test results showed that 65% and 75% burner NO_x reduction efficiencies were achieved on the PC combustor and the tunnel furnace respectively.

The pilot scale simulated NO_x recycle tests were performed on a 1.7 MW cyclone furnace at the B&W Research Center in parallel with the POC tests, since the POC plant did not include the NO_x recycle. The test facility at B&W is a small boiler simulator (SBS). It simulates commercial units very well. The test objective was to investigate parametric effects and provide scale-up information for the commercial plants. The varied parameters were the amount of NO_x fed into the combustor, the injection location (the primary air (PA) alone, the secondary air (SA) alone, and PA and SA simultaneously), the gas compositions (NO, NO_2, and a mixture of NO/NO_2), the furnace load and the excess O_2 concentration.

Figure 3 shows a typical test result for NO injection into the primary air duct at two furnace loads (4 and 6 MBtu/hr) and three exit O_2 concentrations (2%, 3% and 4%). In the figure, R* is the normalized NO_x production rate which is defined as the difference between the stack NO_x with NO_x injection and the injected NO_x divided by the baseline stack NO_x without NO_x injection. All the data shown in Figure 3 fall in a straight line. The linear correlation obtained by the least square method is $R^*=1-0.66\ F^*$. The plot of the normalized NO_x production rate (R*) versus normalized NO_x feed rate (F*) also indicates the burner NO_x reduction efficiency which can be derived as the slope of the straight line. In this case, the burner NO_x reduction efficiency is 66%. When the amount of injected NO increases, the net NO_x production rate in the furnace decreases, but the NO_x reduction efficiency is the same. This linear relationship implies that the reduction of NO_x in the burner might be of first-order kinetic reactions.

All the tests consistently showed that[6]

1) the burner NO_x reduction efficiency was not affected by the amount of NO_x injected or the furnace load;
2) increasing exit O_2 concentration decreased burner NO_x reduction efficiency when NO_x was injected into the secondary air duct;
3) higher burner NO_x reduction efficiency was obtained for the NO_2 injection compared to NO injection. The injected NO_2 was partially destroyed and partially converted into NO in the furnace. Little NO_2 was found in the flue gas for the NO_2 injection tests;
4) injection location had significant effect. The highest burner NO_x reduction efficiency was achieved when NO_x was injected with primary air alone. The lowest burner NO_x reduction efficiency occurred when NO_x was injected with secondary air alone. The burner NO_x reduction efficiency for simultaneous injection of NO_x in both primary air and secondary air followed a nearly linear relationship with the percentage of NO_x injected with primary air.

Correlations can be made from the test data and will be used for the design of the NOXSO commercial plants.

Overall System NO_x Removal Efficiency

The overall system NO_x removal efficiency is affected by the NO_x adsorption efficiency and the burner NO_x reduction efficiency. The relationship among these three efficiencies is easily determined from the material balance. A schematic diagram illustrating the NO_x flow and recycle from the adsorber to the combustor is shown in Figure 4. In the combustor, F mole/hr of NO_x is fed into it from the NO_x recycle stream and R mole/hr of NO_x is produced from combustion. The amount of NO_x leaving the combustor in the combustion gas is:

$$R + F = R_0 + (1-E_3)F \tag{5}$$

where, E_3 is the burner NO_x reduction efficiency and R_0 is the NO_x production without recycle, i.e., baseline NO_x emission. After adsorption, the quantity of NO_x emitted to the atmosphere is given as follows:

$$(1-E_2)\,[R_0 + (1-E_3)F] \tag{6}$$

where, E_2 is the efficiency of adsorption.

$$E_2 = \frac{F}{R_0 + (1-E_3)F} \tag{7}$$

The overall system NO_x removal efficiency (E_1) is evaluated by:

$$E_1 = 1 - \frac{(1-E_2)\,[R_0 + (1-E_3)F]}{R_0} \tag{8}$$

Equation (8) can be rearranged as:

$$E_1 = \frac{E_2 E_3}{1-E_2(1-E_3)} \tag{9}$$

This relationship is illustrated by Figure 5. It shows that the overall system NO_x removal efficiency increases with the NO_x adsorption efficiency and the burner NO_x reduction efficiency. Equation (9) can be used to predict the overall system NO_x removal efficiency for the design of a commercial plant. For example, if the NO_x adsorption efficiency is designed for 90% and the burner NO_x reduction efficiency is 55%, the overall system NO_x removal efficiency will be 80%.

Conclusions

The successes of all the tests during the development of the NOXSO Process has proven that the process can very effectively reduce NO_x emissions from flue gas in addition to the reduction in SO_2 emissions. High overall system NO_x removal efficiency can be achieved by designing a high NO_x adsorption efficiency at a moderate burner NO_x reduction efficiency. Data from pilot scale tests may now be used to design a commercial-scale plant with a minimal level of technical risk.

Acknowledgements

NOXSO Corporation wishes to thank the following for their commitment of personnel and funds to the successful completion of the NOXSO pilot-scale tests: The U.S. Department of Energy's Pittsburgh Energy Technology Center, the Ohio Coal Development Office, Ohio Edison Company, W.R. Grace & Co.-Conn. and MK-Ferguson. The efforts made by the B&W Research Center, who was the subcontractor for the NO_x recycle tests, are also acknowledged.

References

1. Haslbeck, J.L., Wang, C.J., Tseng, H.P., and Tucker, J.D., "Evaluation of the NOXSO Combined NO_x/SO_2 Flue Gas Treatment Process", NOXSO Corporation contract report submitted to U.S. DOE, Report No. DOE/FE/60148-T5 (Nov. 1984).
2. Haslbeck, J.L., Ma, W.T., and Neal, L.G., "A Pilot-Scale Test of the NOXSO Flue Gas Treatment Process", NOXSO Corporation Cooperative Agreement submitted to U.S. DOE, Contract No. DE-FC22-85PC81503 (June, 1988).
3. Yeh, J.T., Drummond, C.J., Haslbeck, J.L., and Neal, L.G., "The NOXSO Process: Simultaneous Removal SO_2 and NO_x from Flue Gas", presented at the Houston, Texas Spring National Meeting of the AIChE (March 29-April 2, 1987).
4. Ma, W.T., Haslbeck, J.L., Neal, L.G., and Yeh, J.T., "Life Cycle Test of the NOXSO SO_2 and NO_x Flue Gas Treatment Process: Process Modeling", Separations Technology, vol. 1, 195-204 (1991).
5. NOXSO Corporation, "Proof-Of-Concept Testing of the Advanced NOXSO Flue Gas Cleanup Process", NOXSO Corporation Final Report to U.S. DOE-Pittsburgh Energy and Technology Center, Contract No. DE-AC22-89PC88889.
6. NOXSO Corporation, "An Experimental Study of NO_x Recycle in the NOXSO Flue Gas Cleanup Process", NOXSO Corporation Final Report to U.S. DOE-Pittsburgh Energy and Technology Center, Contract No. DE-AC22-91C91337.

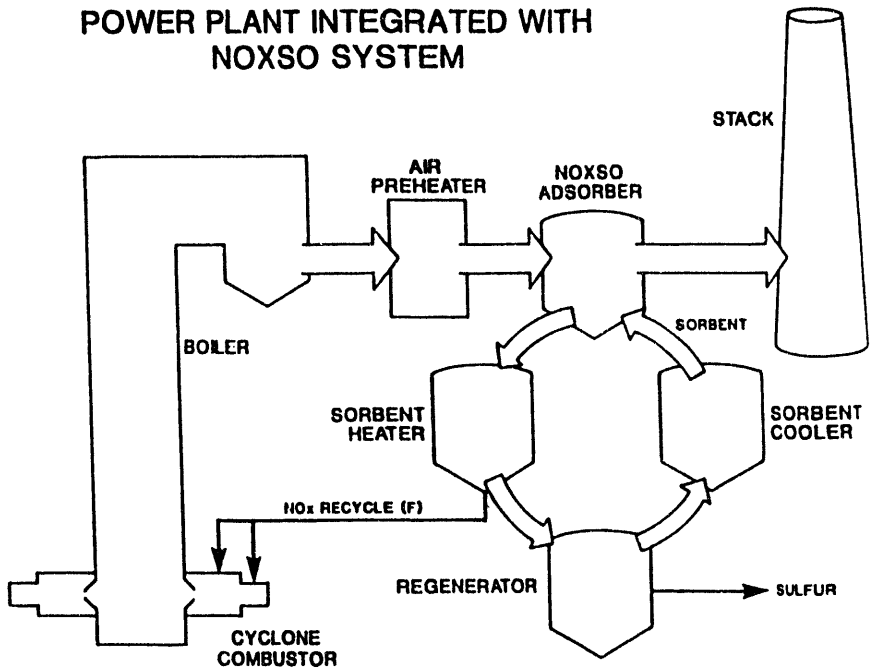

Figure 1. Schematic of the NOXSO Process

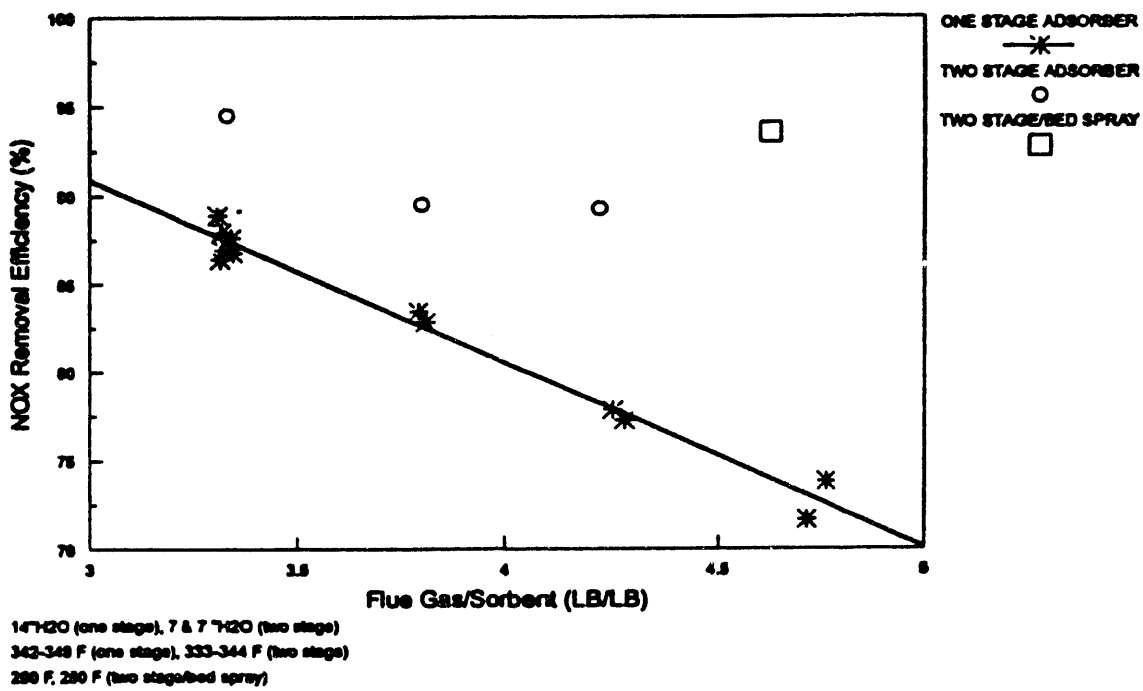

Figure 2. NOXSO Pilot Test One-Stage vs Two-Stage Adsorber

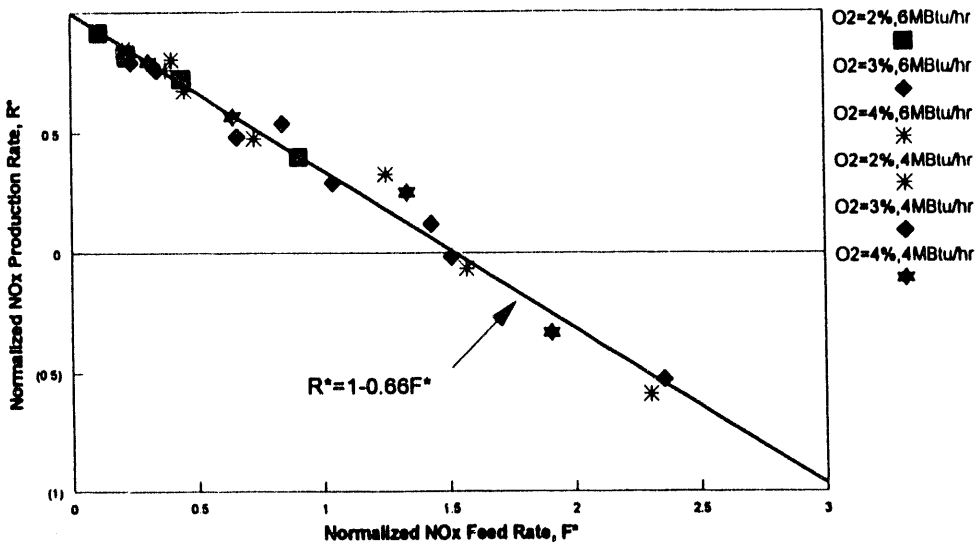

Figure 3. Test Data of NO_x Recycle on B&W's Cyclone Furnace (NO Injection into Primary Air Duct)

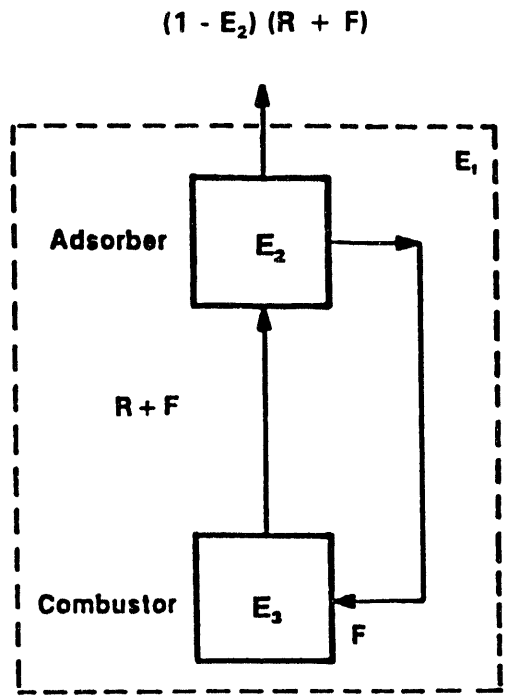

Figure 4. Schematic Diagram of Nitrogen Oxide Recycle

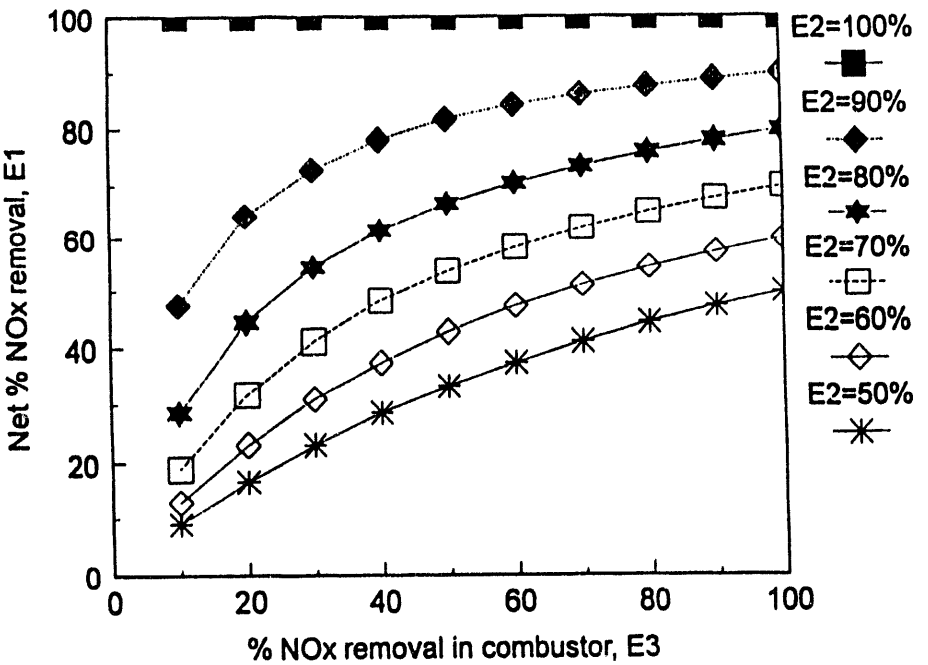

Figure 5. Percentage NO_x Removal in Combustor